

instituto
imdea
nanociencia

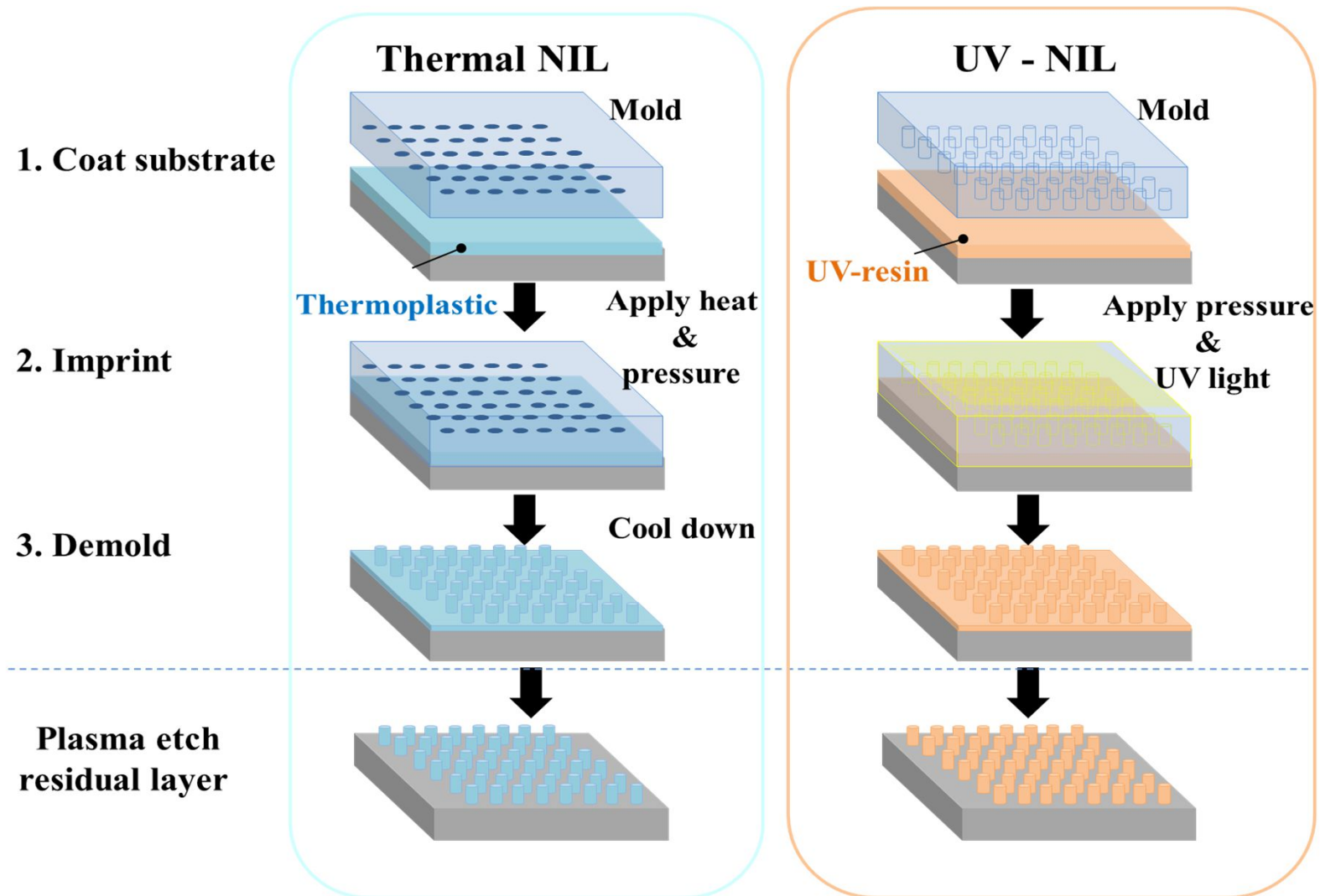


Functional soft-nanoimprinted surfaces

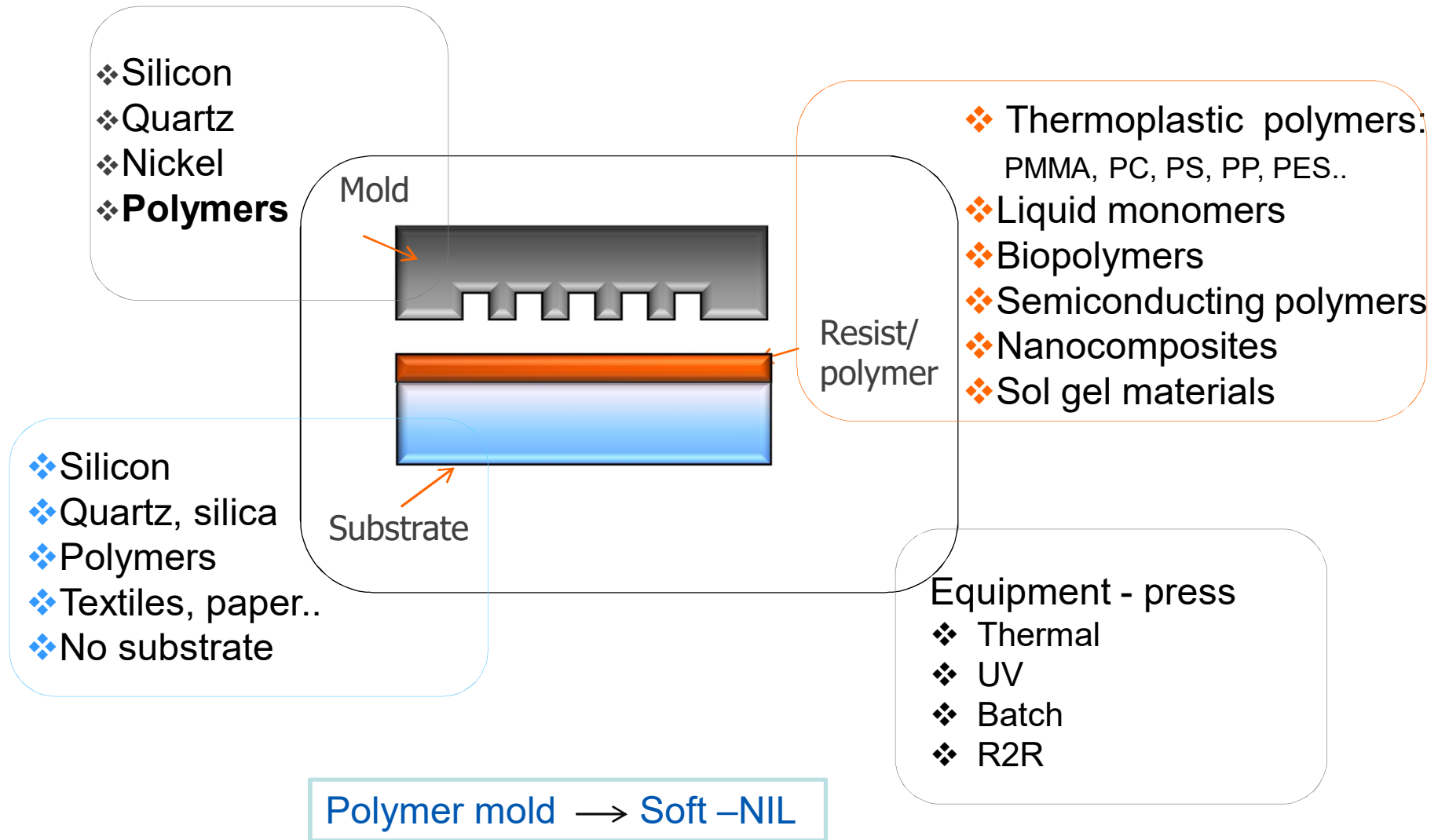
Isabel Rodríguez
i.rodriguez@imdea.org

Nano Imprint Lithography - NIL

A replication process : Pattern transfer by mechanical deformation of a resist material



NIL tool box

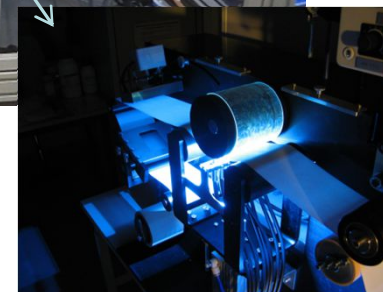


Nanoimprinting machines

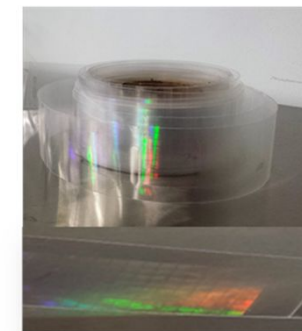
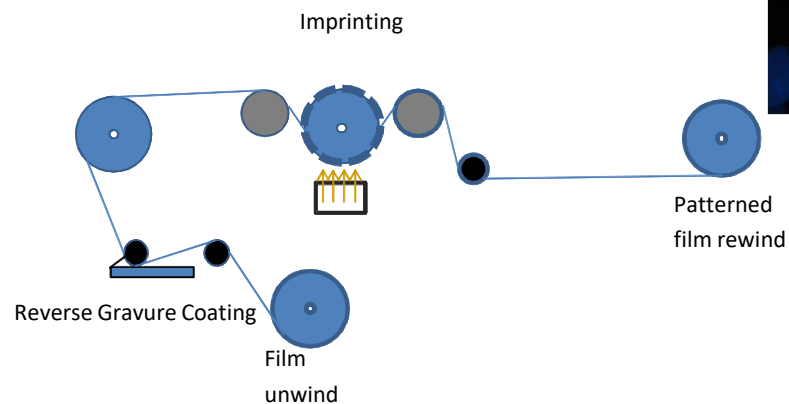
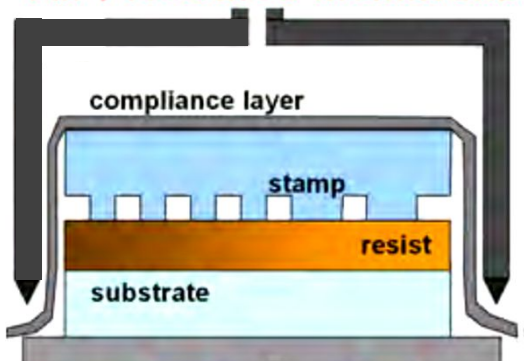
Batch



Roll to Roll

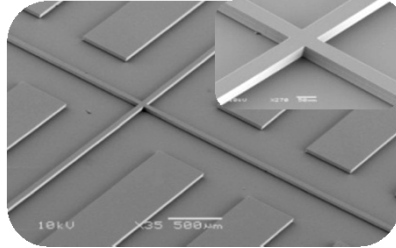


Air Pressured Membrane

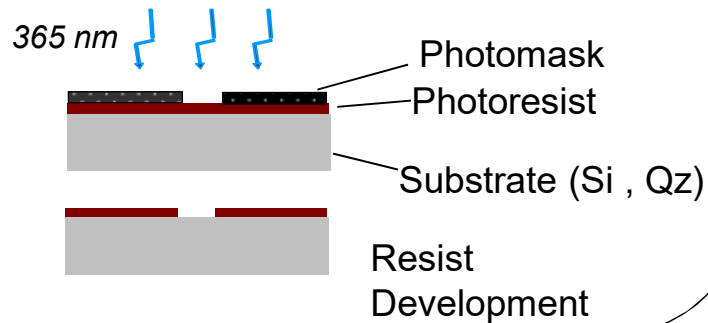


Mold fabrication

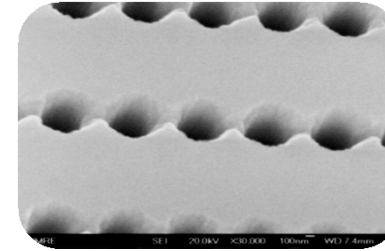
Photo lithography : Micrometer range



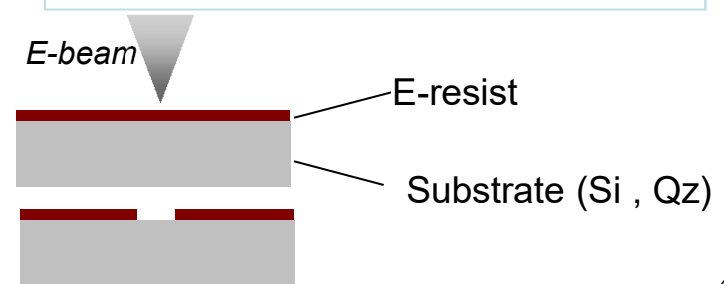
- Limited resolution to 1 μm^2
- Patterned area – 2 - 12"



E-Beam lithography: Sub-micron and Nanometer range



- Resolution from 600- 5 nm
- Limited writing area



Deep Si Etching "Bosch" Plasma process



Working mold
Replication

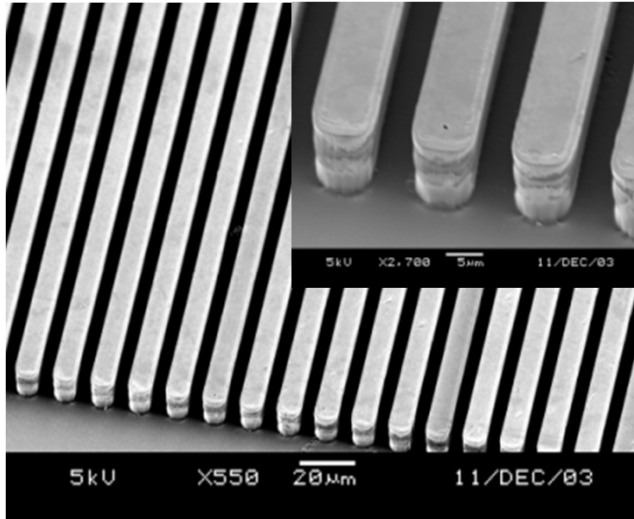


Ni Electroplating

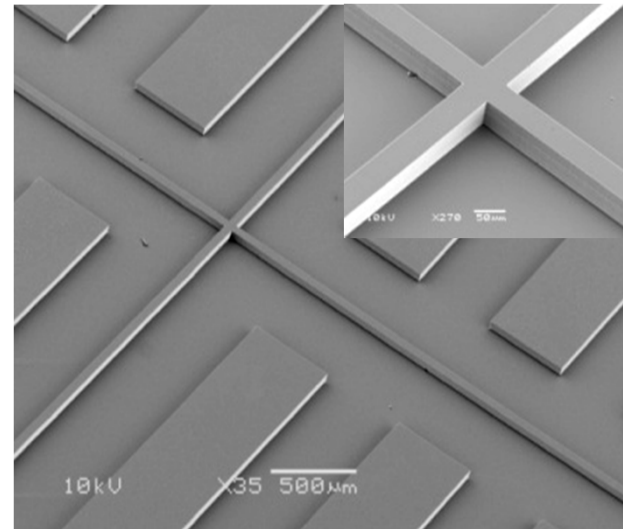
Polymers: PDMS, PFPE ...

Molds - stamps

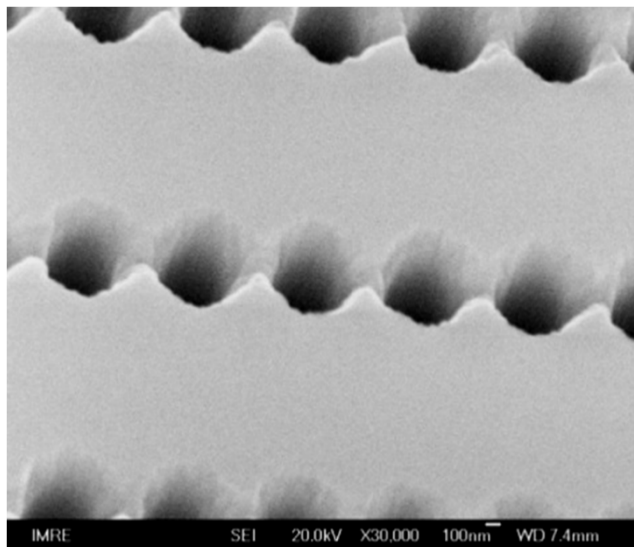
Quartz



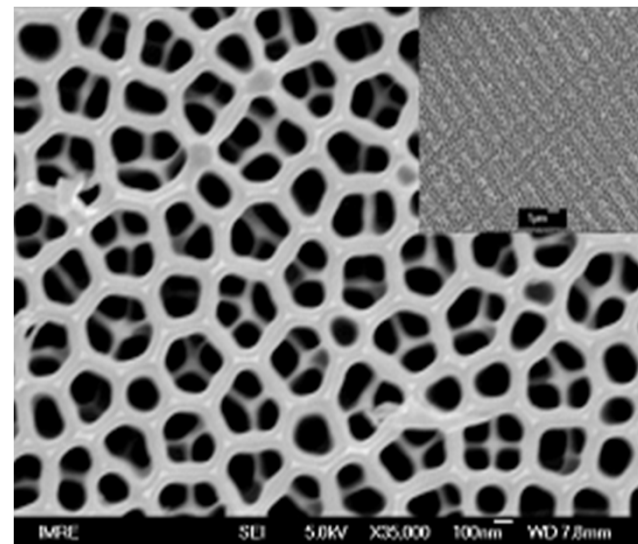
Silicon



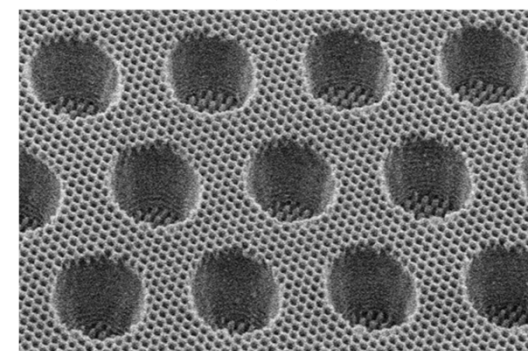
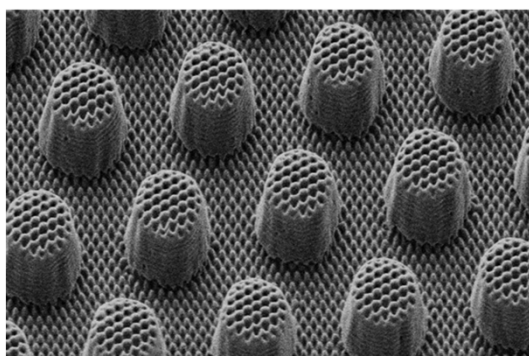
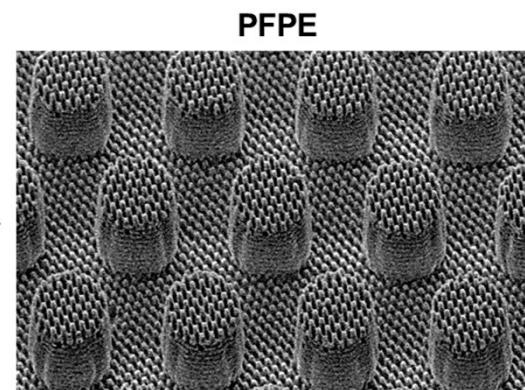
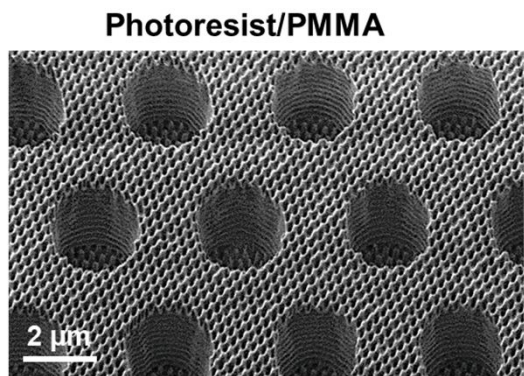
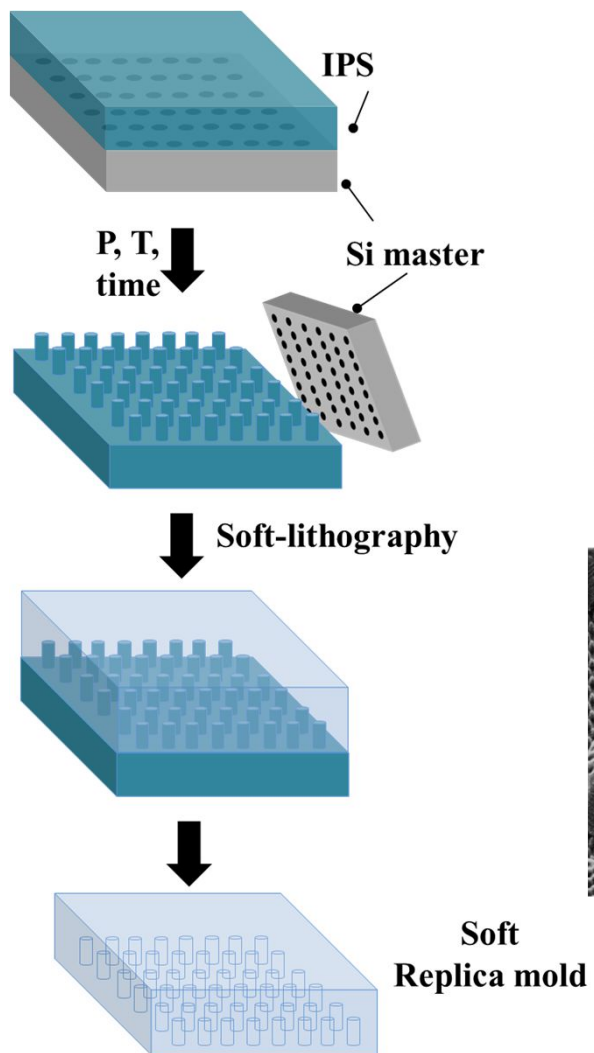
PDMS



Alumina



Soft -NIL



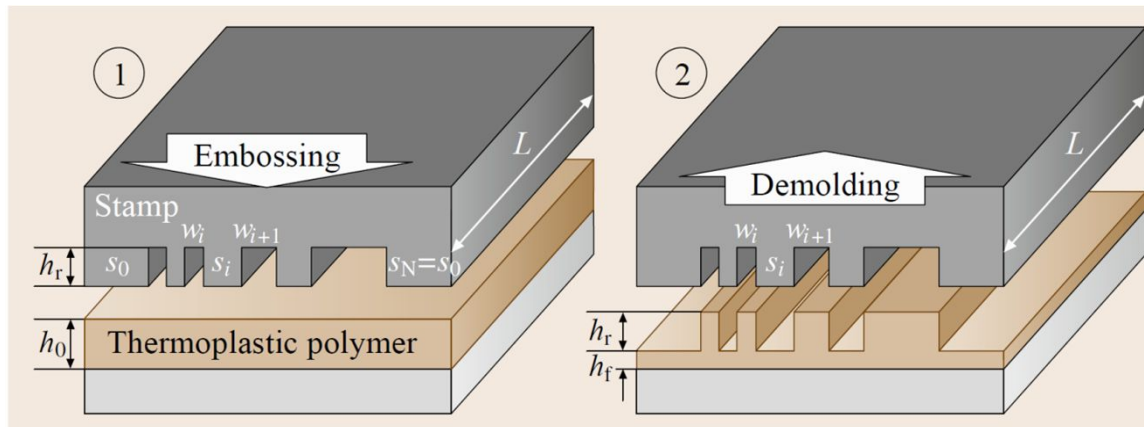
IPS- Intermediate polymer stamp

Nanoimprinting process

Mechanical displacement of (polymer) material by pressure:

1. External pressure: Thin film squeeze flow
2. Laplace pressure: Capillary action

1. Thin film squeeze flow: The polymer flow into the stamp protrusions



Stefan's equation:

$$t_f = \frac{\eta_0 s^2}{2 p} \left(\frac{1}{h_f^2} - \frac{1}{h_0^2} \right)$$

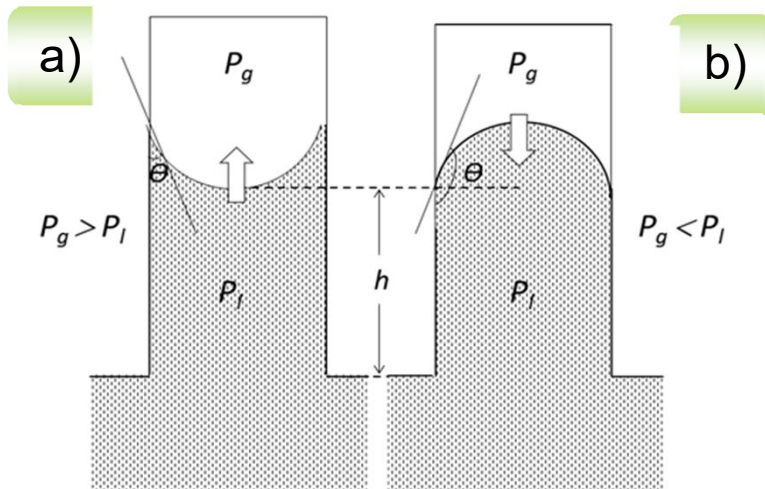
viscosity η_0 stamp width s
 pressure p initial polymer height h_0
 final polymer height h_f

High Aspect Ratio NIL

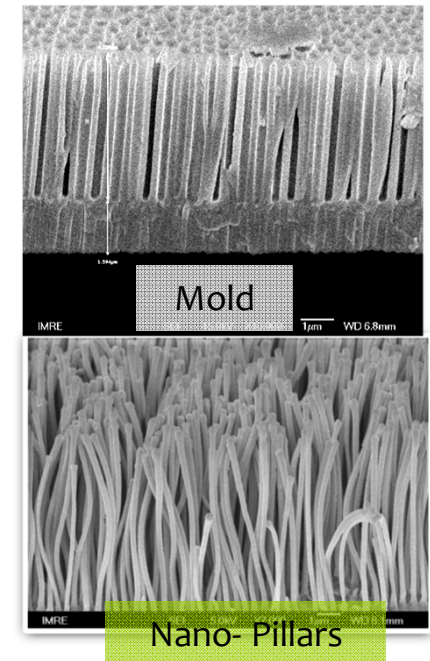
2. Laplace pressure : Capillary action



$$\Delta P_c = P_g - P_l = \frac{2 \gamma \cos \theta}{r}$$



- a) polymer wets the capillary ($\theta < 90^\circ$)
- b) polymer does not wet the capillary ($\theta > 90^\circ$)



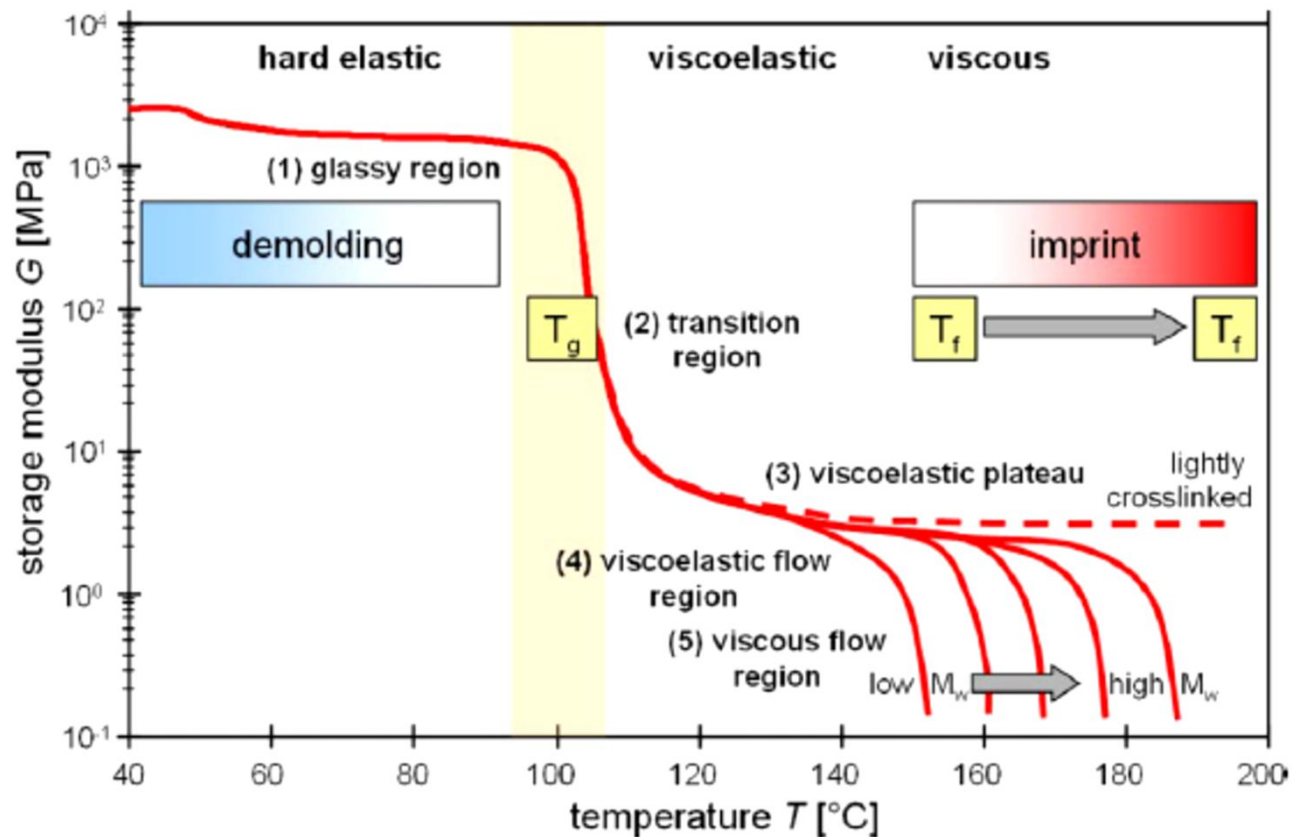
Lucas-Washburn equation:

$$\frac{dh}{dt} = \frac{r \gamma \cos \theta}{4 \eta h} \quad t = \frac{2 \eta h^2}{r \gamma \cos \theta}$$

γ_p is surface tension of the viscous polymer
 η is the viscosity
 θ is the solid-liquid contact angle
 r is the capillary radius.

Choice of process temperature

Mechanical properties of thermoplastics change with temperature

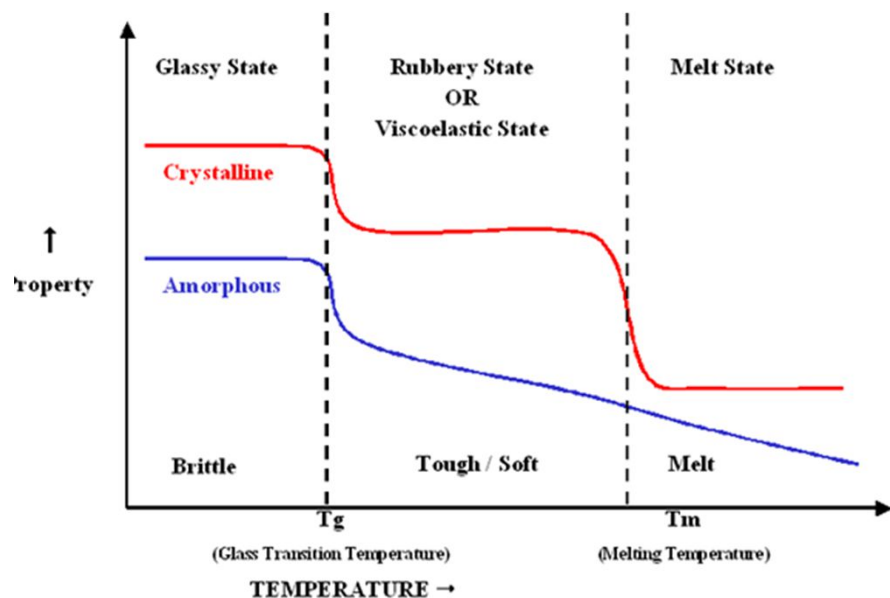
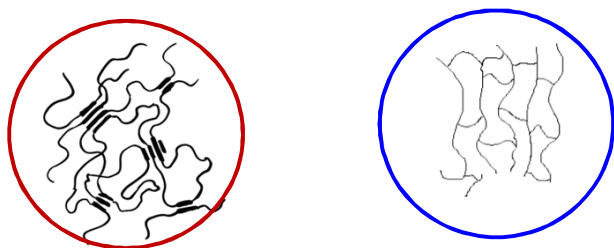


$$T_f = T_g + 50 \text{ C}$$

Optimum viscosity : $10^3 - 10^7$ Pa.s

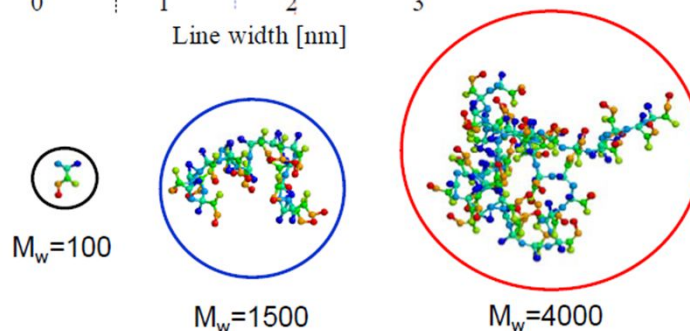
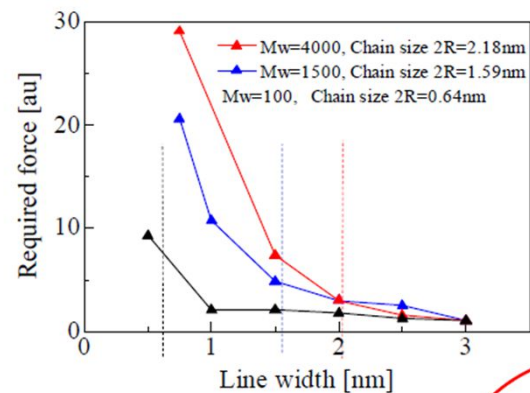
The imprint material – critical resolution

Thermal phase transitions Crystalline vs amorphous



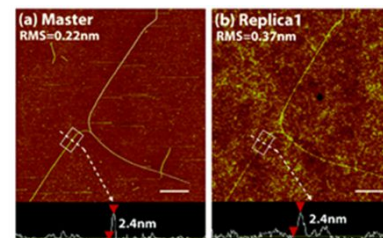
<http://injectionmoldingonline.com/Molding101/Polymers.aspx>

Molecular weight



Y Hirai et al, *J. Vac. Sci. Technol. B* 2010, **28**, C6M68

Ultimate Resolution -1 nm

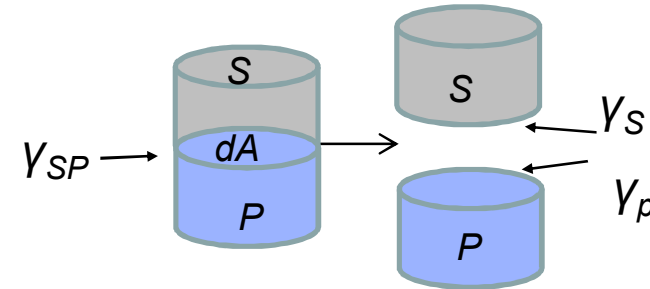


Demolding

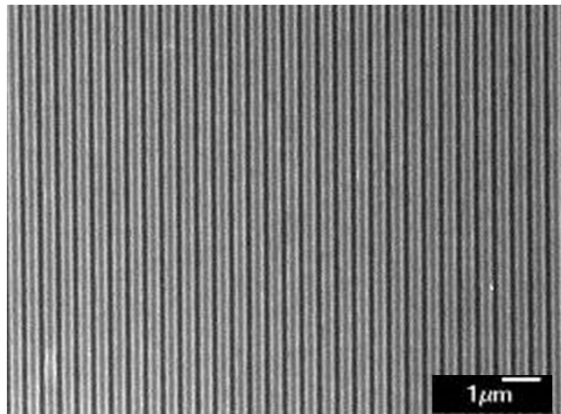
Adhesion + friction forces

Work of adhesion :

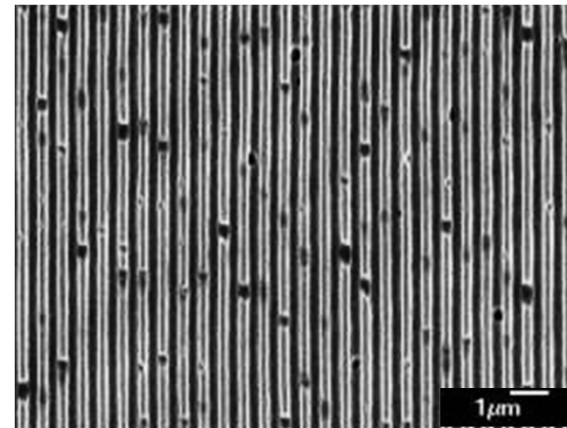
$$dW_{SP} = (\gamma_S + \gamma_P - \gamma_{SP}) dA$$



Mold with anti-stick coating



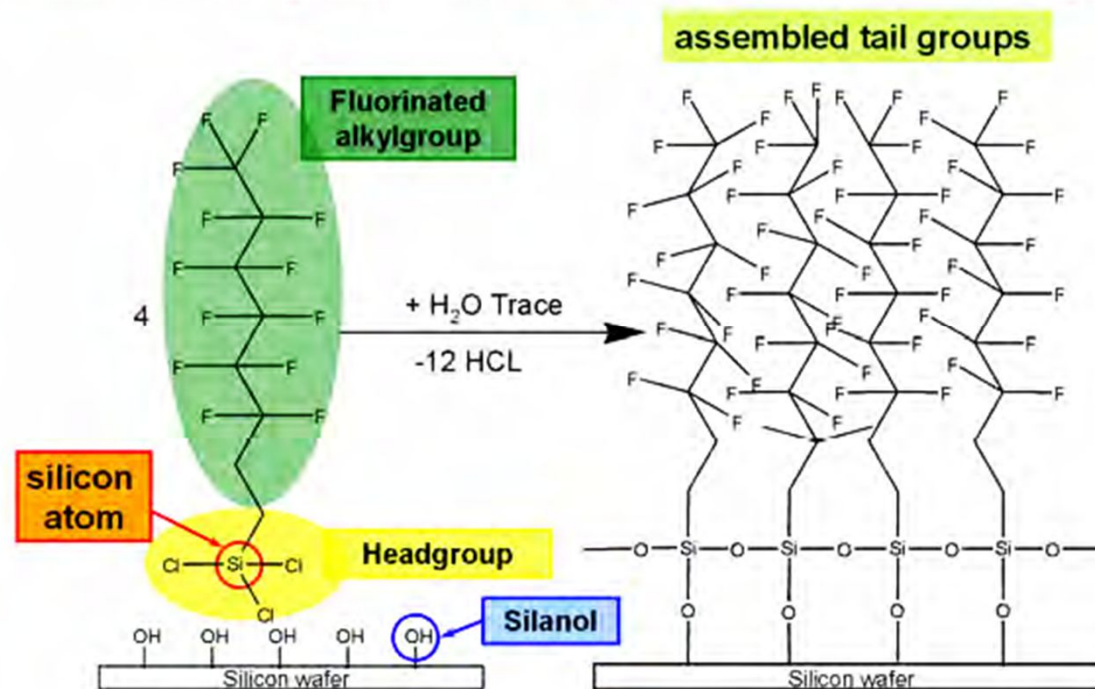
Mold without anti-stick coating



Anti-sticking coatings

Anti-adhesion surface treatment to reduce the surface energy

Fluorinated organosilane as molecular anti-adhesive layer



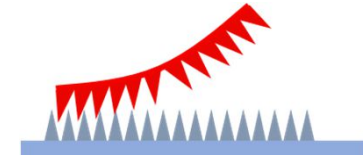
Perfluorodecyltrichlorosilane (FDTS)

Heptadecafluoro-1,1,2,2-tetrahydrooctyl)-trichlorosilane (F13-TFS),

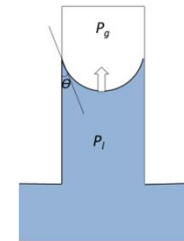
Surface energy values range: $10 \text{ mJ/m}^2 < \gamma_s < 20 \text{ mJ/m}^2$

Advantages of soft-NIL

➤ Sequential action of peeling the mold from substrate



➤ High gas permeability



➤ Conformal contact to substrate



➤ Low surface energy

- ❑ Common thermoplastic polymer used in T-NIL and their processing conditions

Thermoplastic polymer	Young's modulus*	Surface energy	T _g (°C)	T imprint (°C)	Viscosity*	Young's modulus* (MPa)
	(MPa) 25 °C	(mJ·m ⁻²) 20 °C			(mPa·s) T imprint	(MPa) T imprint
PMMA	2500	41.1	100-120	140-190	10 ⁷ -10 ⁴	380-540 (80 °C)
PS	2350	10.7	110	140-190	10 ⁷ -10 ⁵	100 (110 °C)
PC	2270	34.2	150	160-200	10 ⁶ -10 ⁴	438 (160 °C)
						2.18 (170 °C)
PP	1300	30.1	-20 to -10	200	10 ⁶ -10 ³	200 (125°C)
PVDF	1500	30.3	-40 to -35	200	10 ⁴ -10 ³	-

* Molecular weight dependent

- ❑ Common soft mold materials properties

Material	Young's modulus (MPa)	Surface energy (mJ·m ⁻²)	Viscosity (mPa·s)	Resolution (nm)
s-PDMS	1.8 - 2	25	3900	250
h-PDMS	10 - 14	35	< 490 (tunable)	15
PFPE	315	12.7	430	15

Nanoimprinting highpoints

- ♣ **High-resolution** - Not limited by diffraction but by the mold size (1 nm resolution demonstrated)
 - ♣ **High-throughput** - Roll to roll scalable, roll to plate
 - ♣ **Low-cost**
 - ♣ **Versatility** - Material flexibility
Process flexibility : UV, thermal
Feature flexibility : micron- nanoscale
 - ♣ **Low environmental impact** : **Greener** - less use of solvent, developers etc.
-
- ❖ Defects, mold patterning and mold wear
 - ❖ Mechanical resistance of the nanofeatures

Nanofabrication

Nanomanufacturing

Direct writing techniques

Replication techniques

mass fabrication processes

E-beam lithography

Ion beam lithography

Scanning probe lithography

Direct Laser Writing Lithography

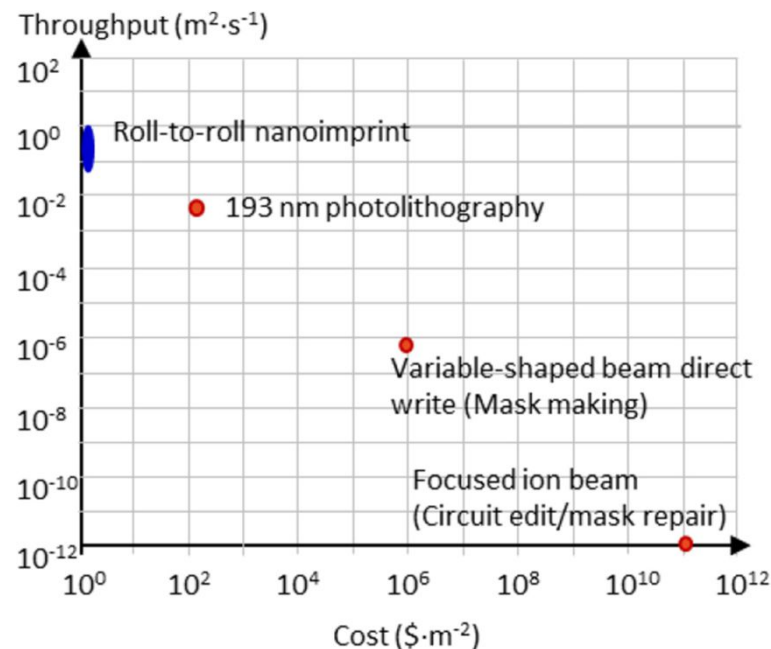
Two-photon Lithography - 3D printing

Optical lithography

X-ray lithography

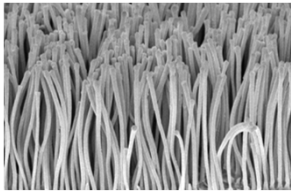
Nanoimprint technology

Resolution ~ Throughput – Cost

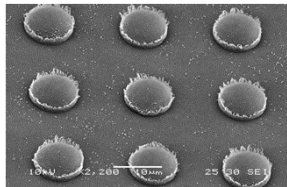


Patterning techniques used in integrated circuit manufacturing.
J. A. Liddle & G. M. Gallatin,
Nanomanufacturing: A Perspective
ACS Nano 2016, 10, 2995.

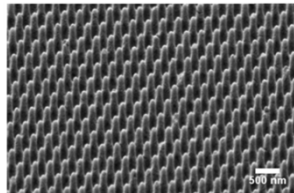
Surface functions & bio-applications



- Gecko like dry adhesives



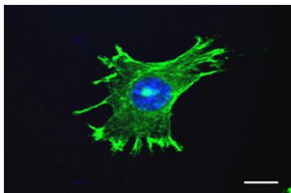
- Superhydrophobic lotus



- Anti-reflective moth-eye



- Bactericidal Moth Eye Inspired Topography

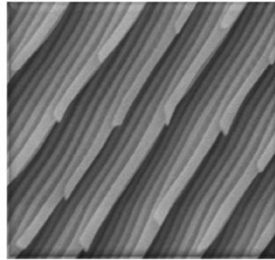


- Cell Instructive Patterned Topographies

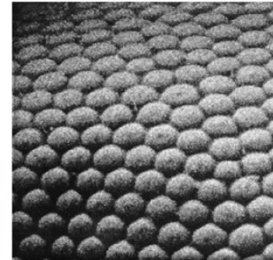
Natural functional surface structures



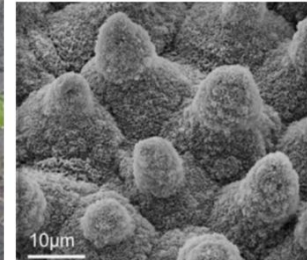
Structural colour



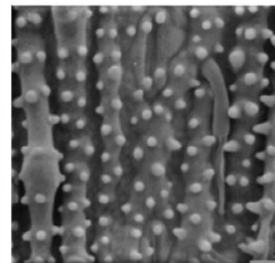
Anti-reflective



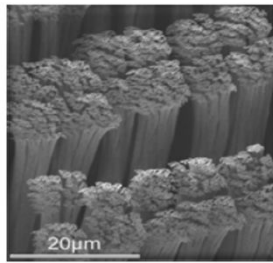
Super hydrophobic



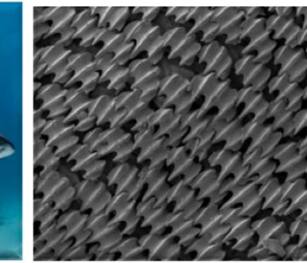
Anisotropic wetting



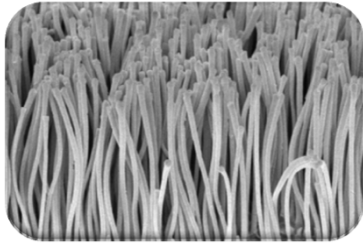
Adhesive



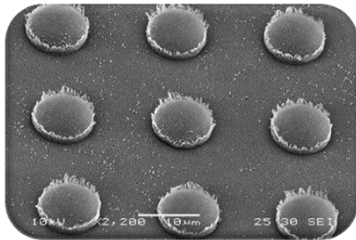
Non adhesive



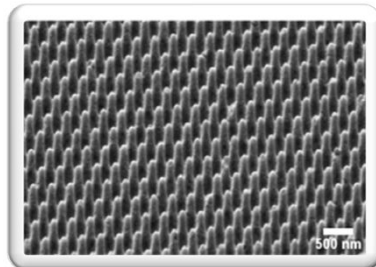
Surface functions & applications



➤ Gecko like dry adhesives



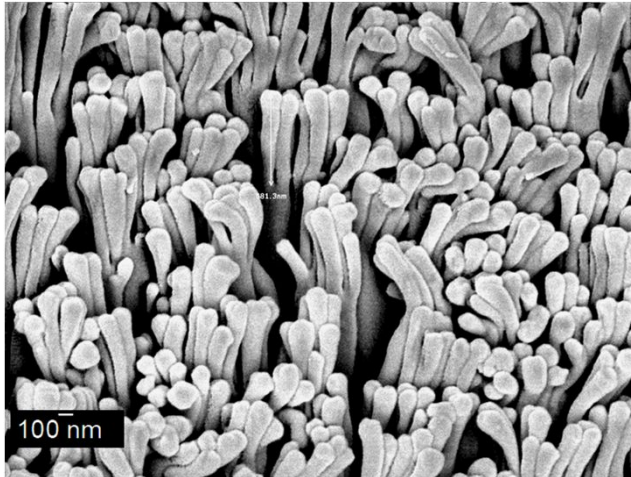
➤ Superhydrophobic lotus



➤ Anti-reflective moth-eye

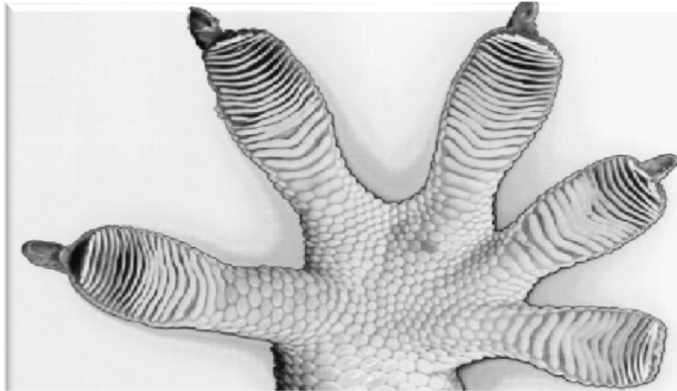
Gecko like dry adhesives

van der Waals adhesion - residue free

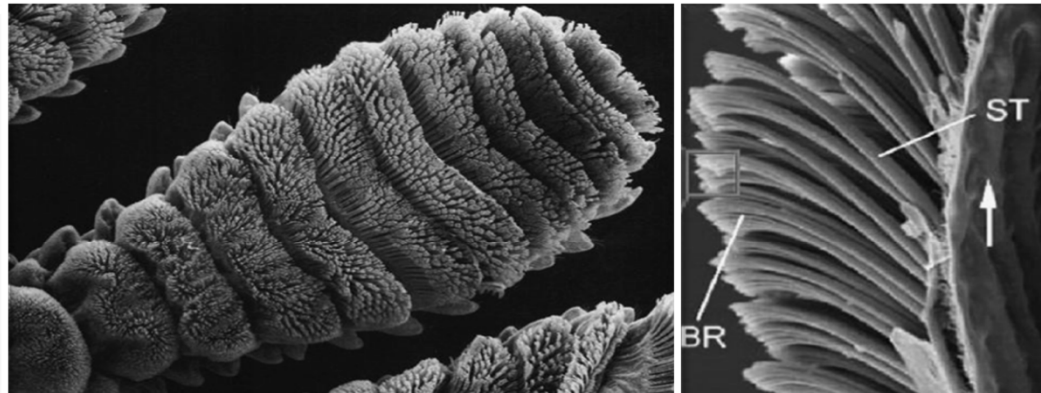


Polymeric
hierarchically
branched fibrils

Gecko's Hierarchical Attachment System



Autumn, K., et al., Nature, 2000. **405**(6787): p. 681.



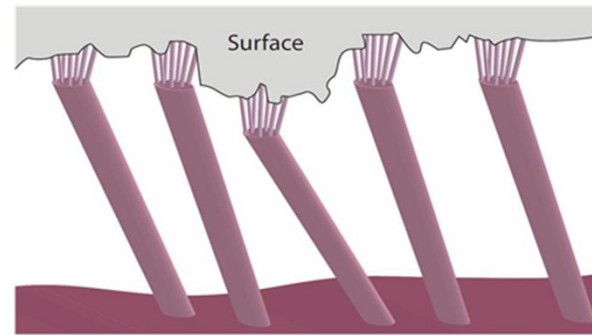
Bhushan, B., J. Adhesion Sci. & Tech., 2007. **21**(12/13): p. 1213.

Hierarchy (β -keratin)	Name	Diameter	Height	Aspect Ratio	Density (#/mm ²)
Level 1	Seta	~ 4 μ m	~ 110 μ m	~ 25	14 x 10 ³
Level 2	Branch	~ 1 μ m	~ 25 μ m	~ 25	-
Level 3	Spatula	~ 100 nm	~ 2.5 μ m	~ 25	1.4 - 14 x 10 ⁶
End of Level 3	Tip of Spatula	Width	Length	Thickness	
		200 -300 nm	500 nm	10 nm	

Hierarchy allows for conformal contact - Adhesion via van der Waals forces

Gecko adhesive hierarchy of compliant structures

Conformational contact to surface roughness

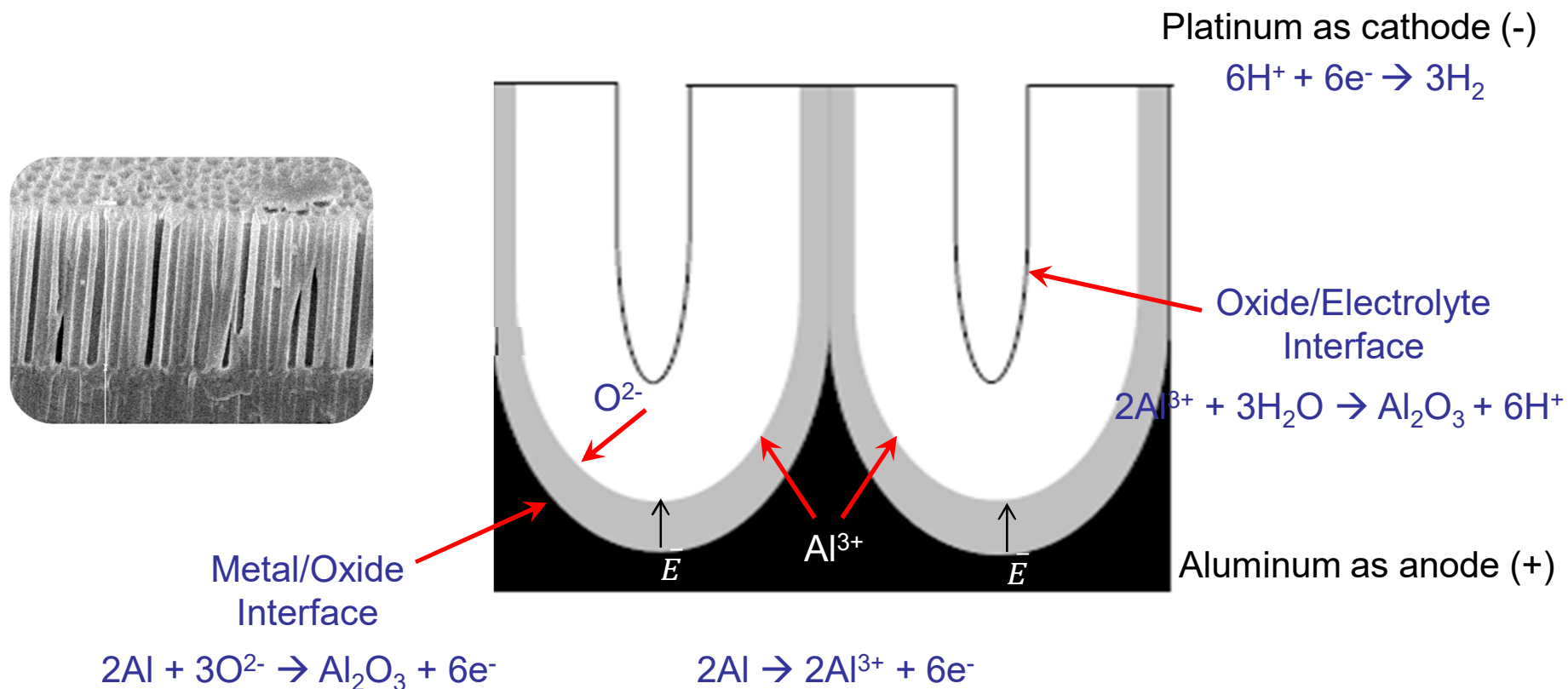


Benchmark functional properties:

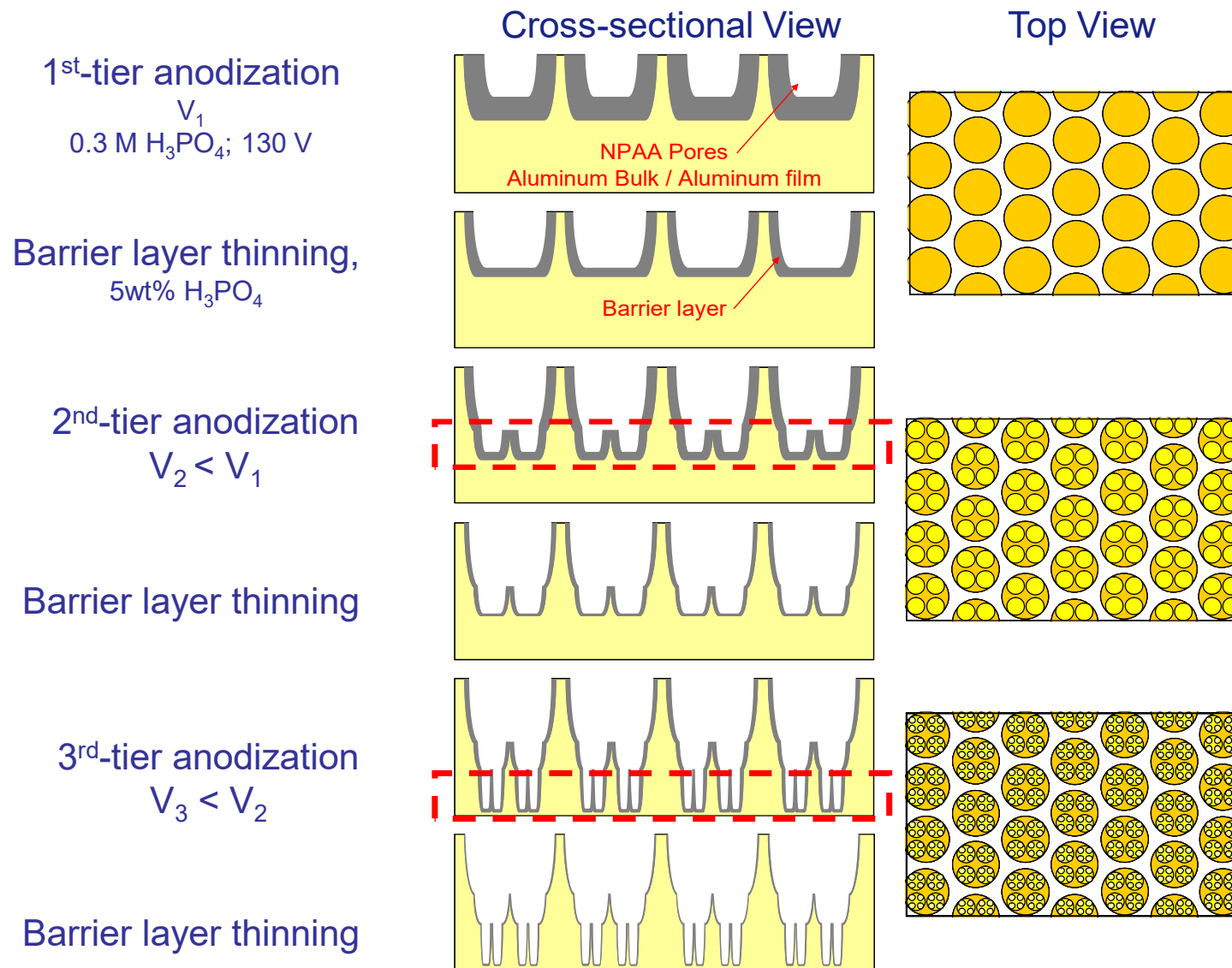
1. Anisotropic , directional attachment - shear force adhesion
2. High pull off to preload ratio
3. Low detachment force
4. Material independence / van der Waals adhesion
5. Self-cleaning
6. Anti-self matting
7. Non-sticky in default state

Mold fabrication: Nano porous alumina

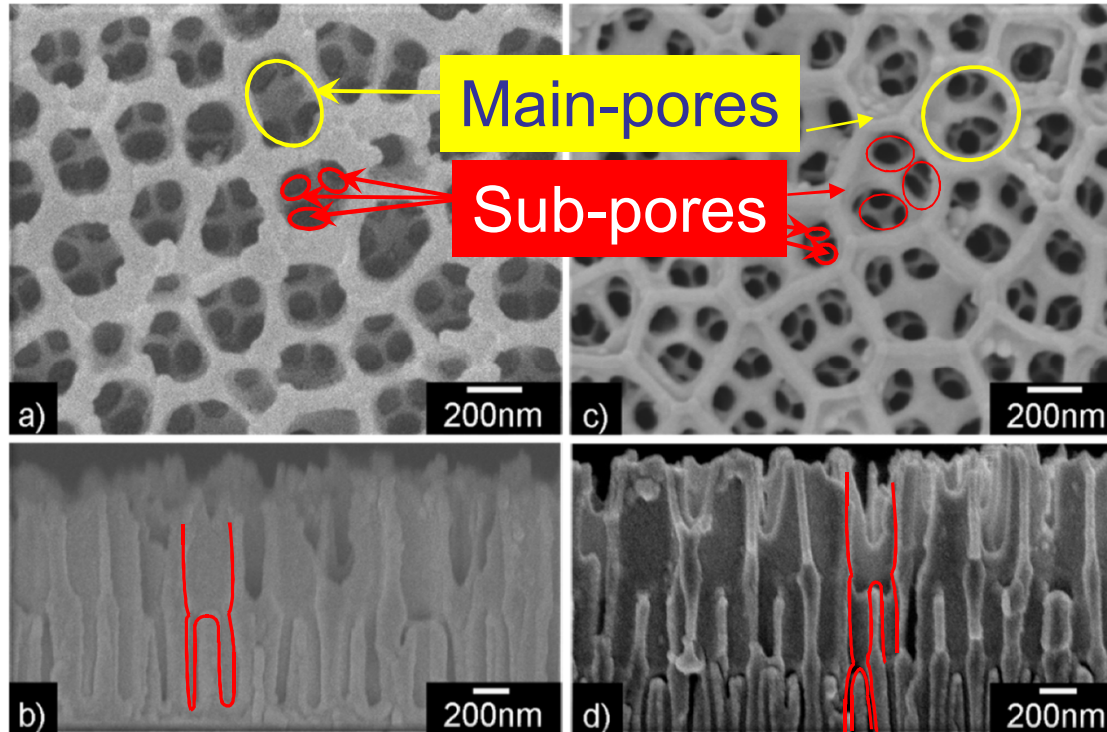
Aluminium anodization - Alumina Pore Formation



Fabrication of hierarchical PAA template

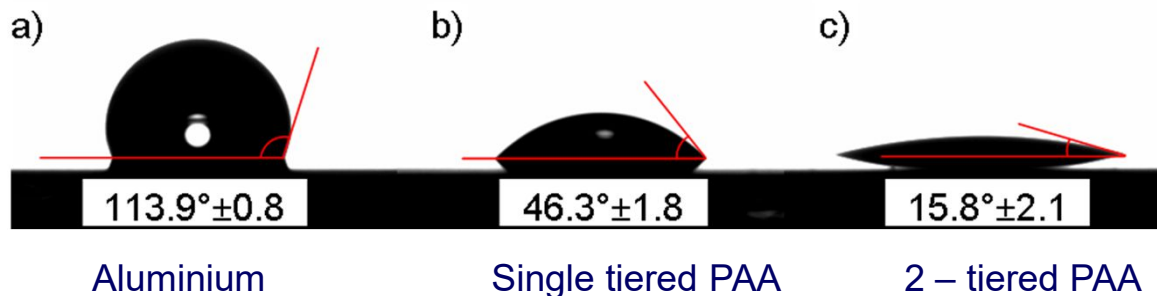
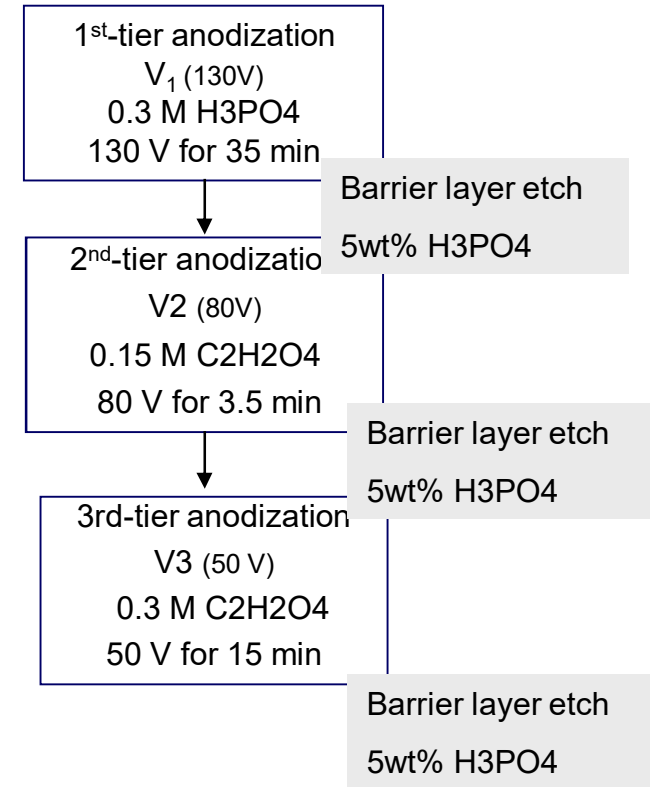


Tiered Branched Porous Alumina Template



Advanced Functional Materials 2008, 18, 2057-2063.

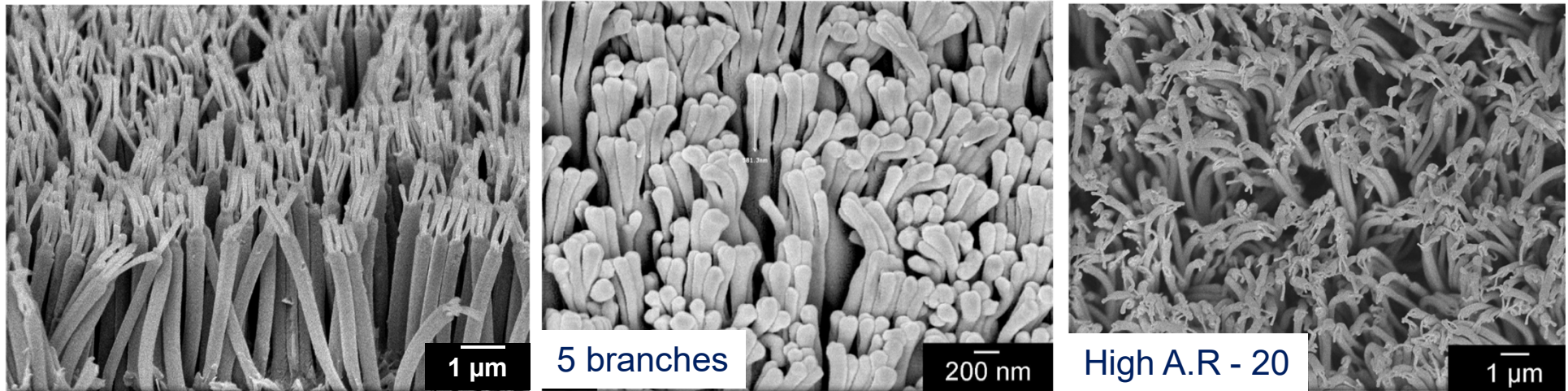
2-3 step aluminum anodization



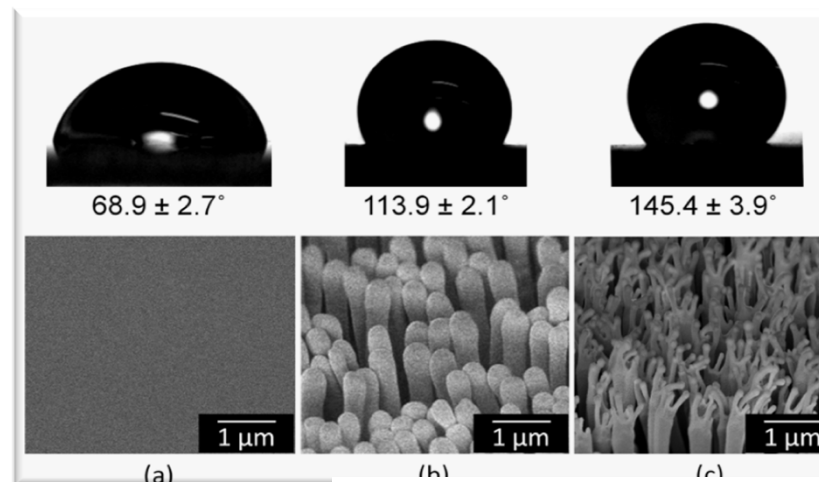
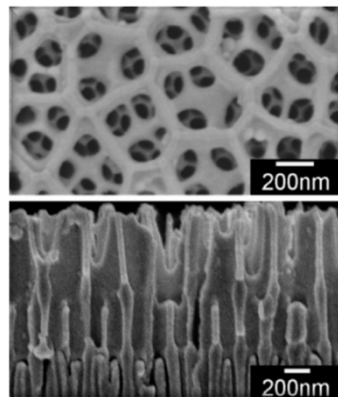
Increased wettability →
- filling of the pores

Hierarchical gecko like dry adhesives

Main fibril's \varnothing : 250 nm , A.R – 10, ρ – 6.2×10^6 fibrils/mm²

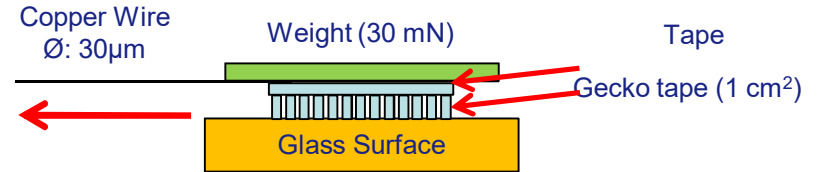
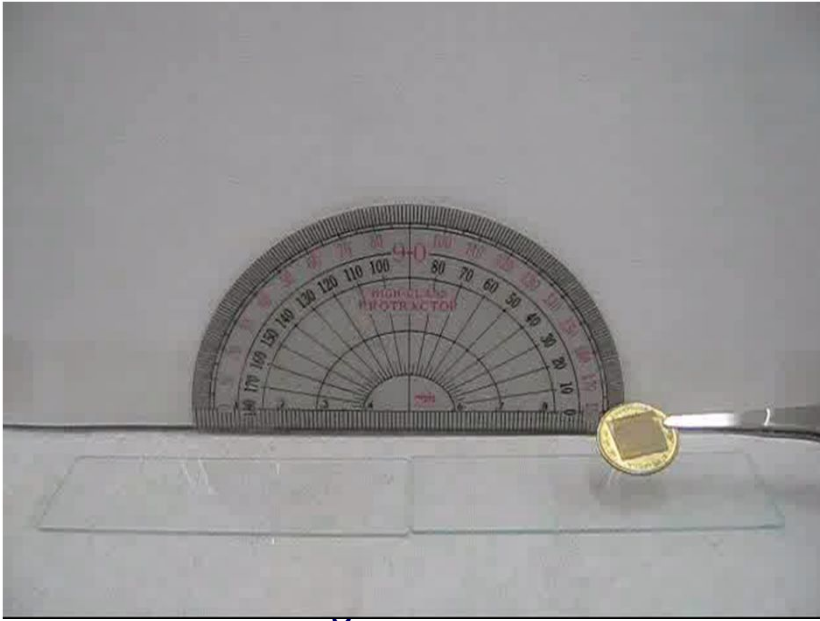


Wetting characteristics

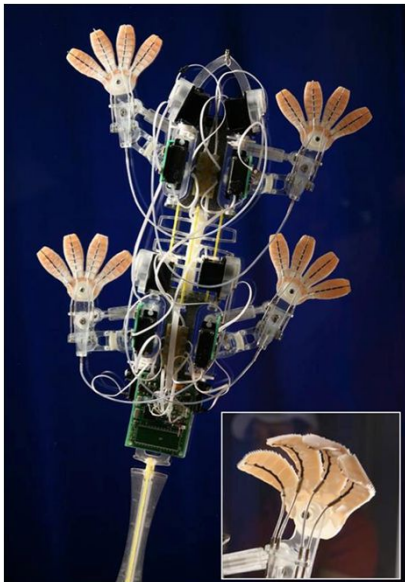


Pristine Polycarbonate Linear pillars Branched pillars

Frictional Adhesion Measurements

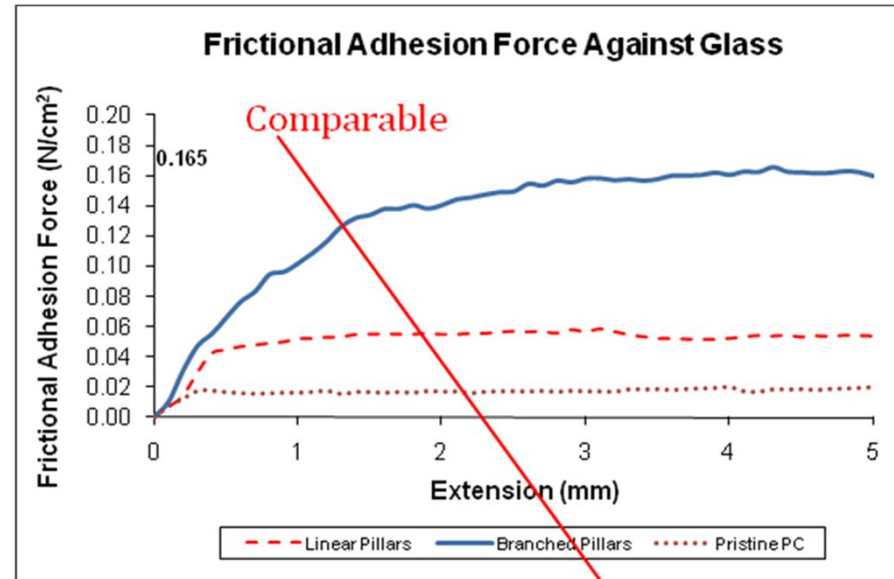


Gecko tape friction test set up



Stickybot

Biomimetic Robotics
Lab , MIT



Values by estimating contact region with preload of 0.03 N/sq.cm.

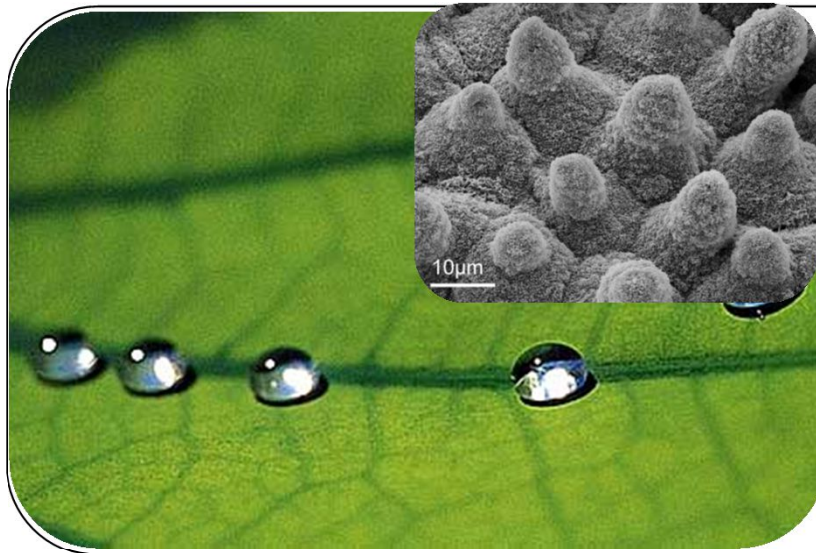
Typical weight of Gekko Gecko : 43.4 ± 1.48 g

Pad area : 2.271 ± 0.109 cm²

→ Frictional Adhesion Force : **0.188 N/cm²**

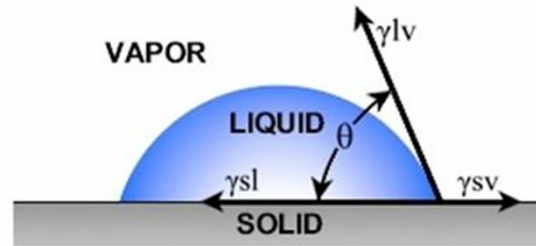
D.J. Irschick et al., *Biological Journal of the Linnean Society* (1996),
59: 21-95.

Superhydrophobic, self cleaning lotus leaf



Hierarchical
micro/nano
topography

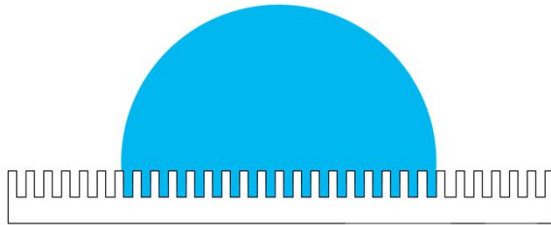
Wetting properties : contact angle



$$\cos \theta_o = \frac{\gamma^{sv} - \gamma^{sl}}{\gamma^{lv}}$$

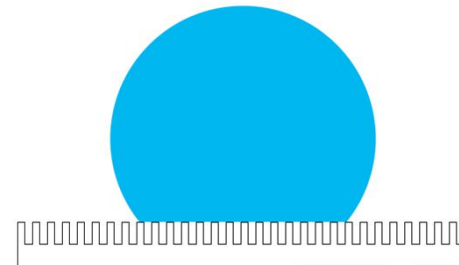
Young's equation

Wenzel state



$$\cos \theta = r \cos \theta_o$$

Cassie- Baxter state



$$\cos \theta = r f \cos \theta_o - 1 + f$$

Super hydrophobic surfaces

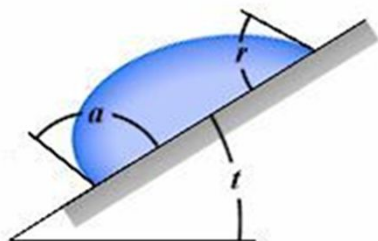
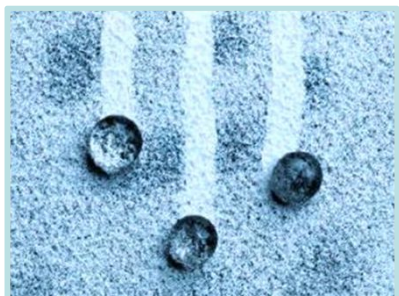
~ Synergy : surface energy + topography ~

Apparent contact angle (θ) above 150°



160°

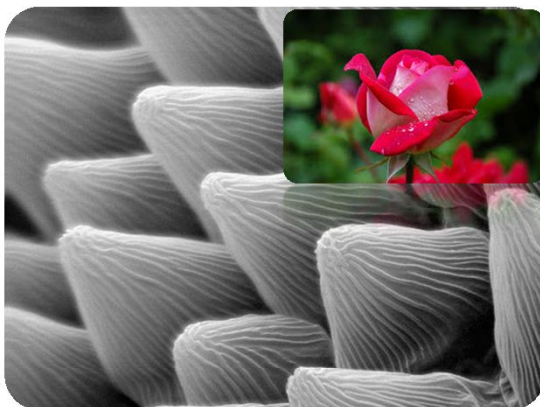
Self-cleaning surfaces



~ Synergy : surface energy + topography ~
 apparent contact angle (θ) above 150°
 + contact angle hysteresis below 10°
 $H = \theta_a - \theta_r$

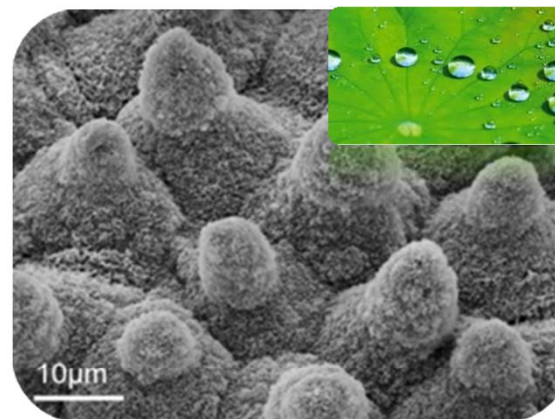
Topography modulated wettability

Self-pinning



Petal (Cassie impregnating wetting state)

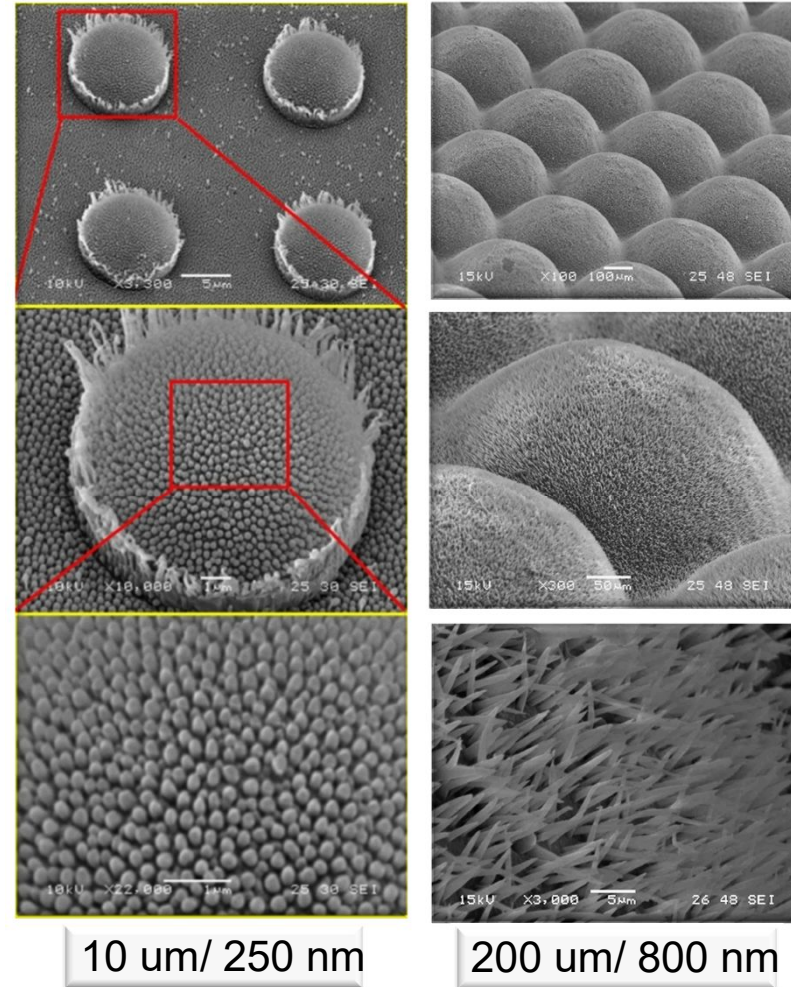
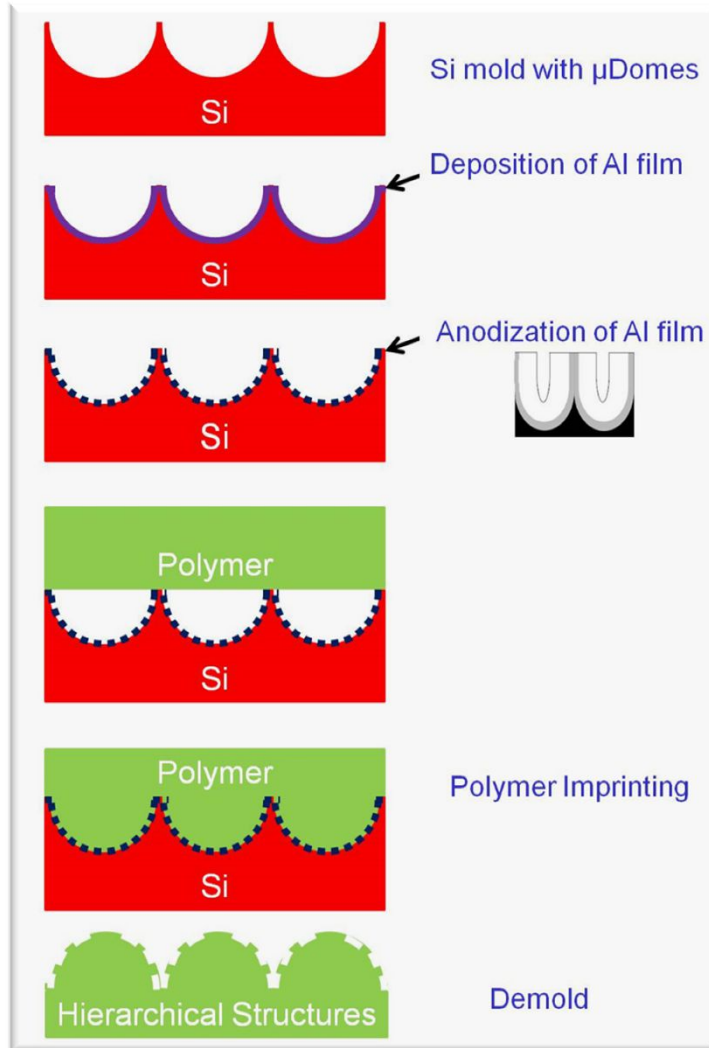
Self-cleaning



Lotus (Cassie's state)

Lotus-like structure fabrication

Fabrication process steps



SHS - Wetting properties

Water
Contact
Angle



113 °

160 °

163 °

Water contact angle on 10 μm / 200 nm hierarchy

Topographies	Static contact angle(deg)		
	Flat	Micro	Hierarchical
Pristine (PP)	103 ± 3	-	-
400 μm / 0.8 μm		104 ± 9.1	153 ± 4.6
10 μm / 200 nm		113 ± 2.4	160 ± 2

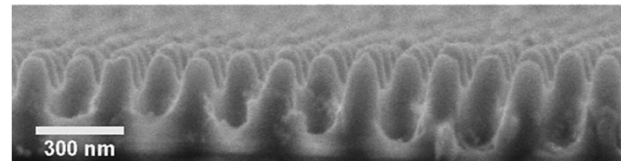
Topographies	Contact angles (deg)		
	Static	Hysteresis	Sliding
400 μm / 0.8 μm	154 ± 0.5	10 ± 4	8 ± 1.7
10 μm / 200 nm	160 ± 2	9 ± 1	4 ± 0.3



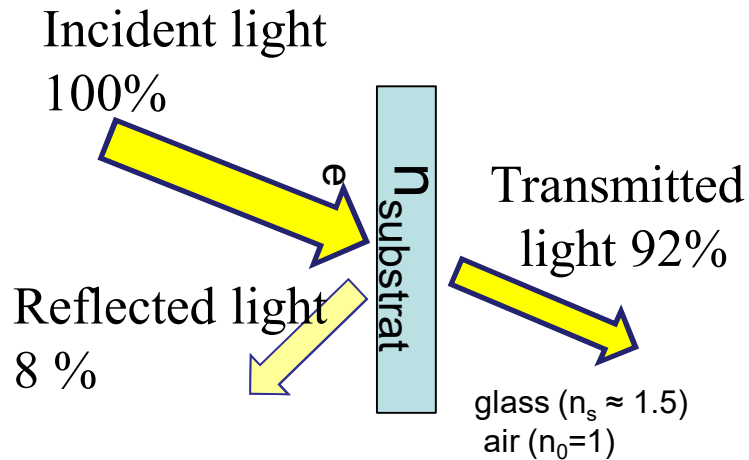
Anti-reflective surfaces



Graded
Refractive Index



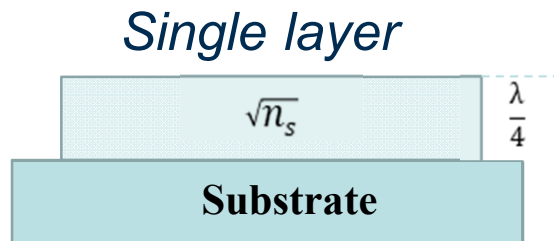
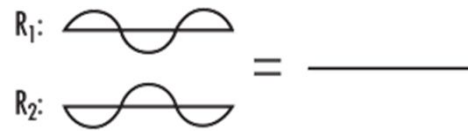
Light Reflection



Fresnel's Equation:

$$R = \left[\frac{n_s - n_0}{n_s + n_0} \right]^2$$

Anti-reflection: destructive interference

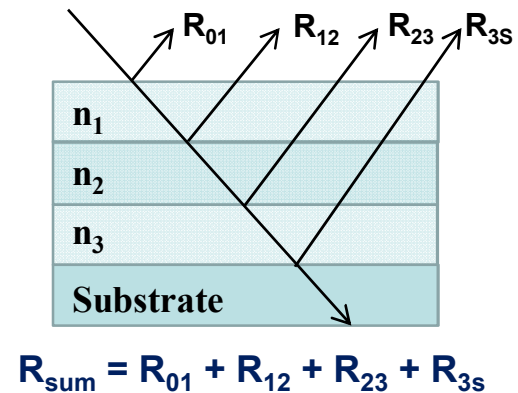


Refractive index for an ideal AR coating:

- (1) $n_c = (n_a n_s)^{1/2}$
 (2) $d = \lambda/4$
- } **Glass** \rightarrow $n_s=1.2$
 MgF₂ (with an index of 1.38)

Few materials and high price!!!

Multiple layer

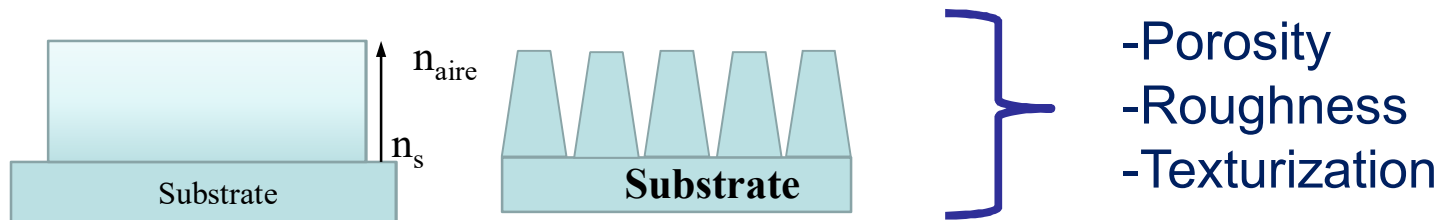


Expensive approach!!!

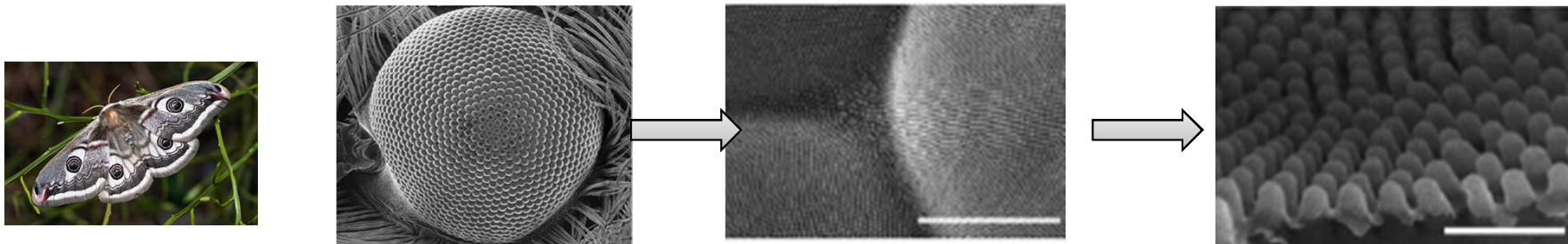
Anti-reflective strategy

Antireflexion: Innovative alternative

Graded refractive index



Moth's eye natural antireflective topography – subwavelength nanocone features



Pros of AR textured surfaces

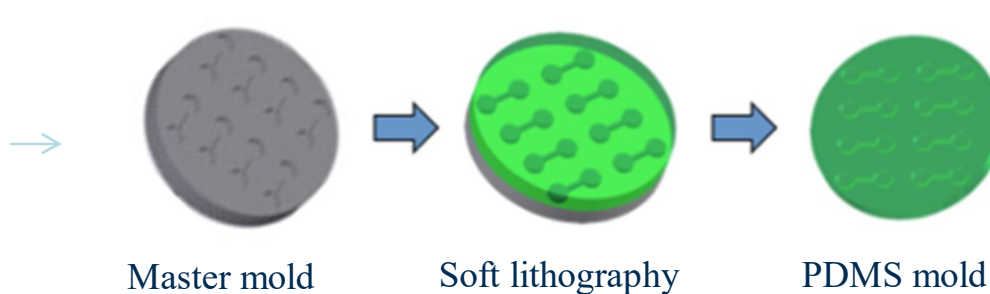
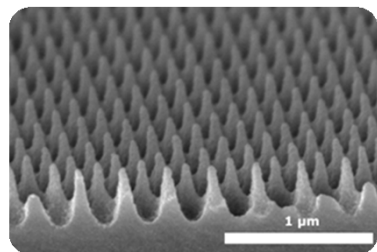
- AR Broad spectral range
- Omnidirectional
- Low cost, scalable ->R2R

Cons of AR textured surfaces

- Poor mechanical behavior
- Cleaning

Moth-eye Nanoimprinting

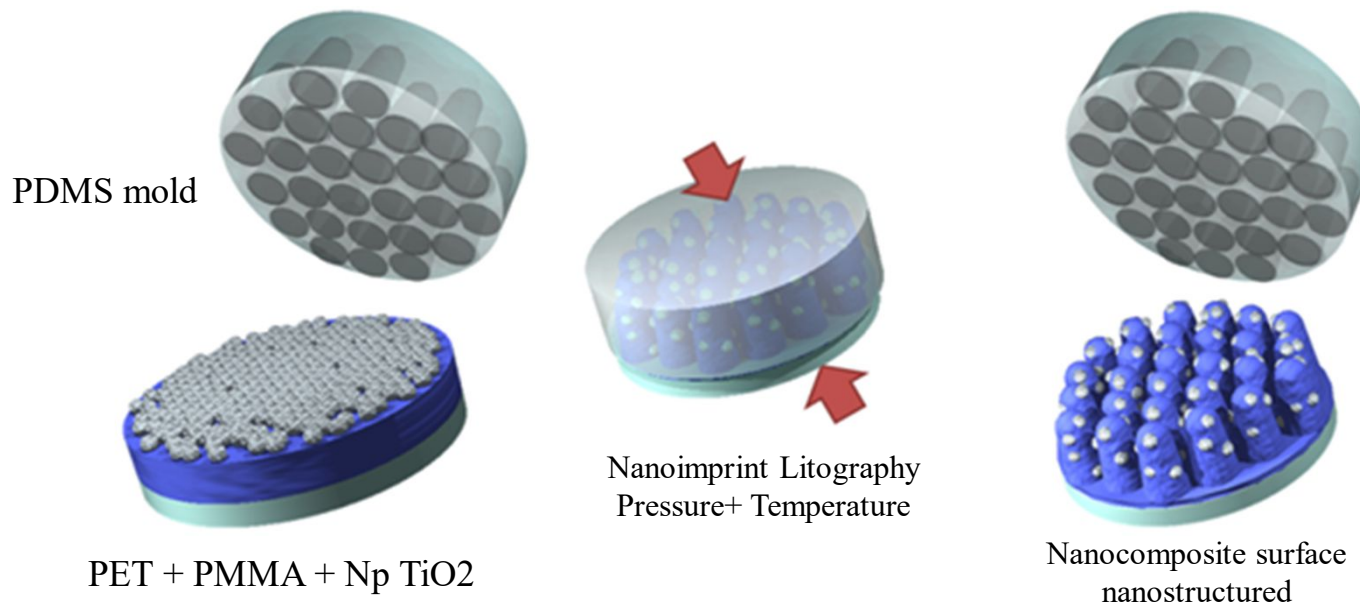
Moth-eye nickel mold replication by Soft lithography



In situ
polimerization
of PDMS

Soft Thermal NIL

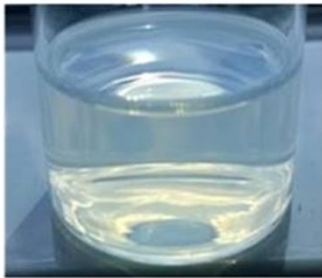
Patterning polymer	PMMA/TiO ₂
Pressure (bar)	45
Temperature (°C)	170
Time (s)	300



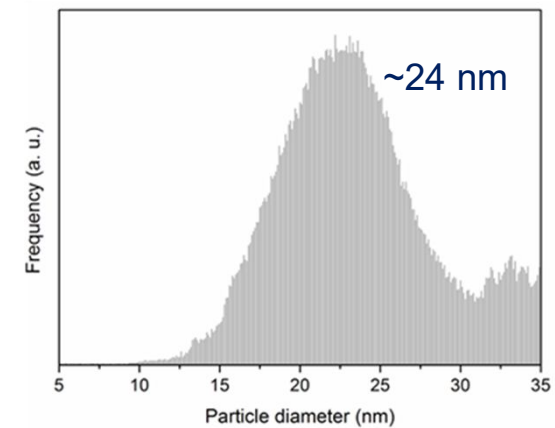
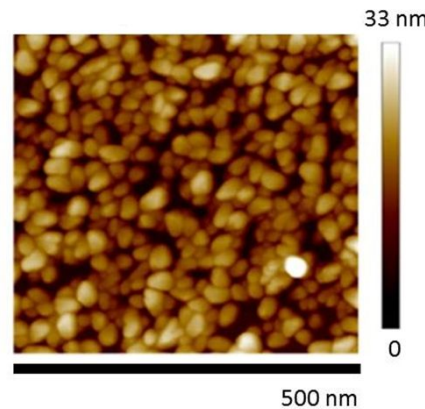
TiO₂ Surface Nanocomposite

Preparation of polymer nanocomposite

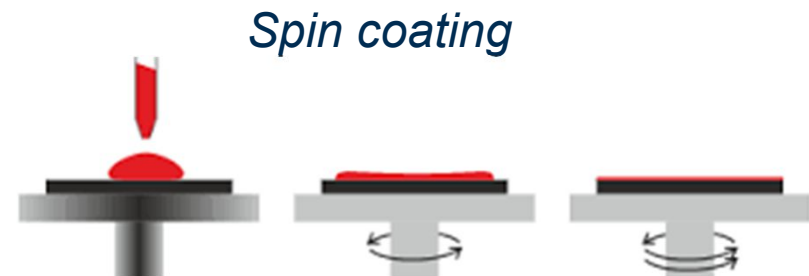
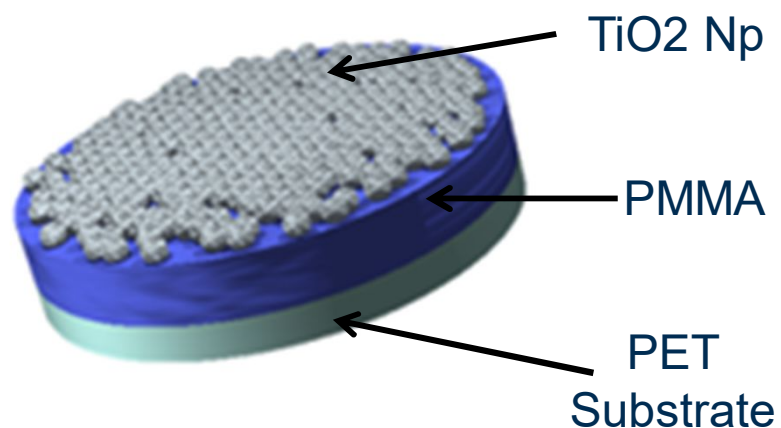
TiO₂ nanoparticles: Hydrothermal synthesis



Colloidal suspension



Nanocomposite preparation

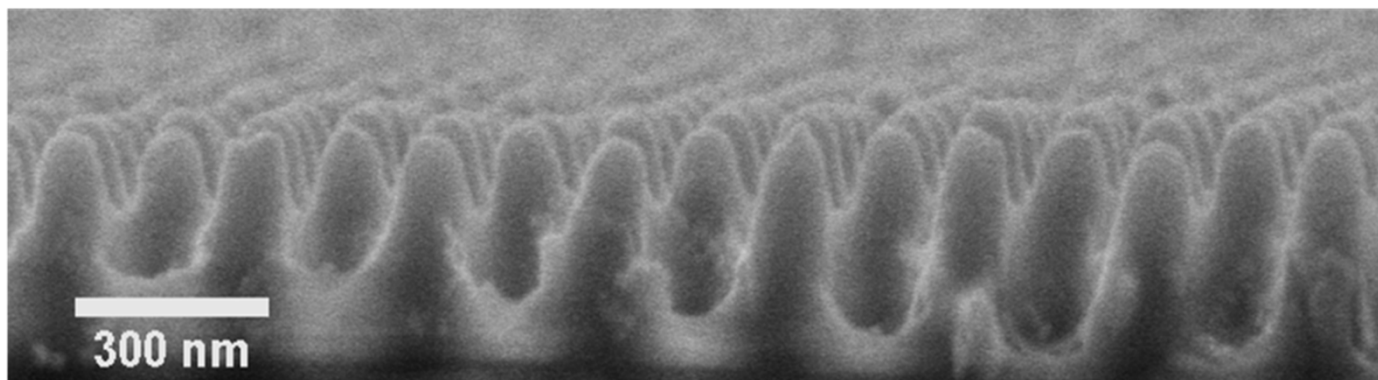
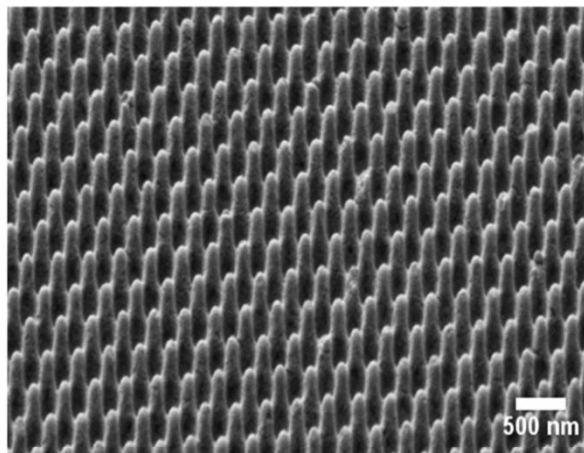
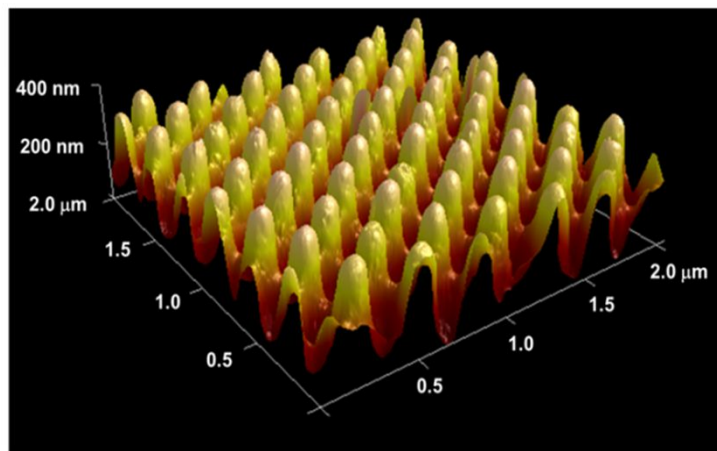


Spin coating

Different amounts
of nanoparticles were
deposited

Moth-eye nanostructures

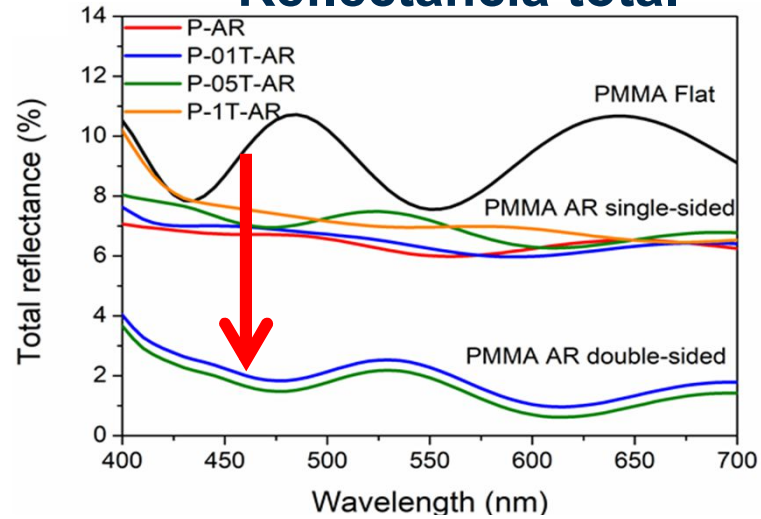
Morphology: SEM & AFM images



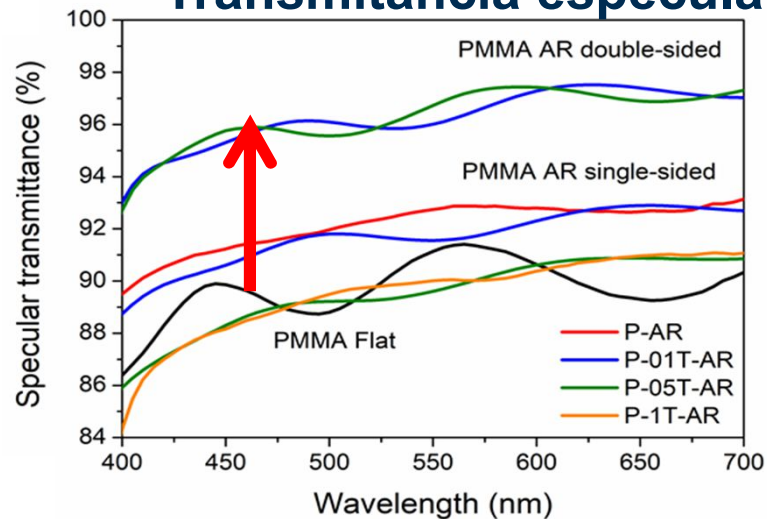
- High fidelity replication of the master mold on PMMA Nanocomposites
- Good nanoparticles dispersion
- Embedded particles within the polymer

Moth-eye optical characterization

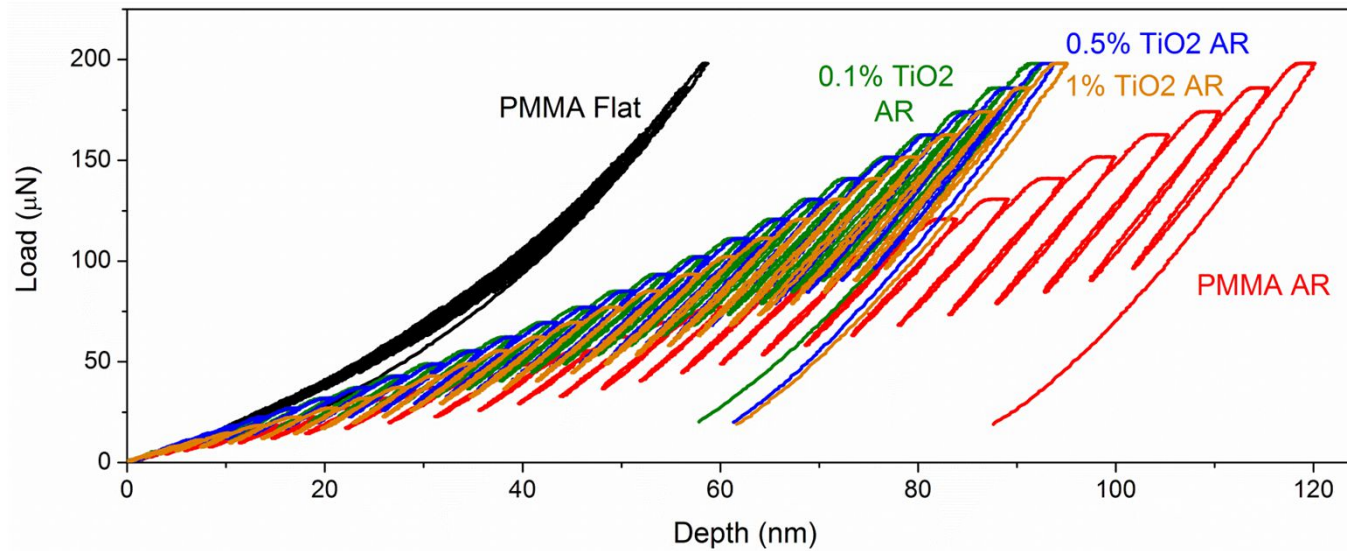
Reflectancia total



Transmitancia especular



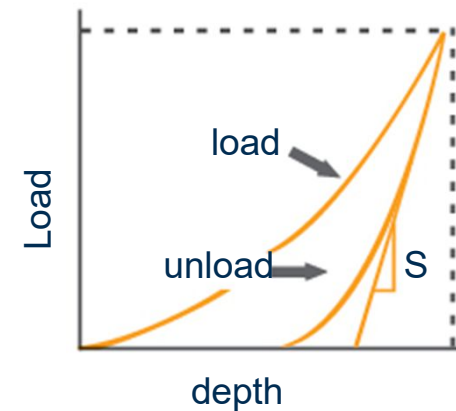
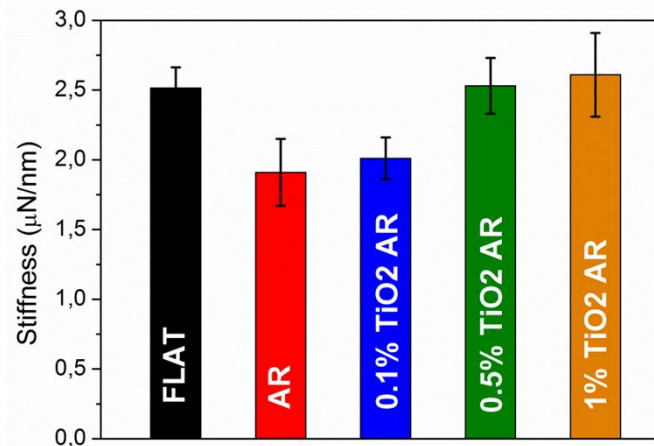
Mechanical behavior: Nanoindentation



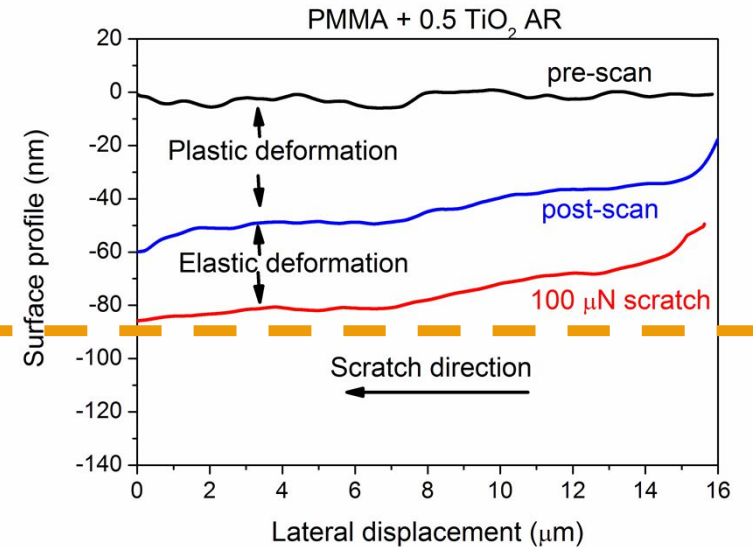
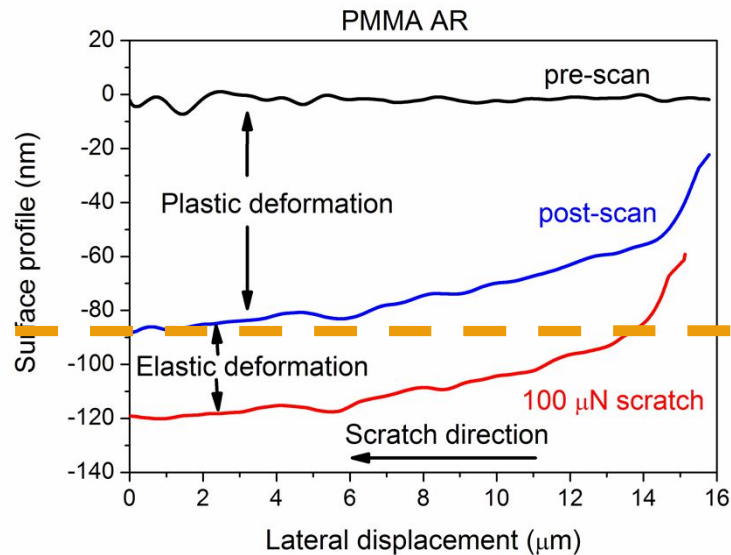
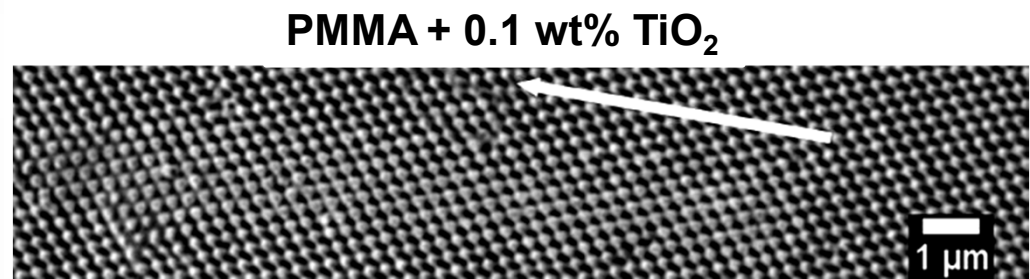
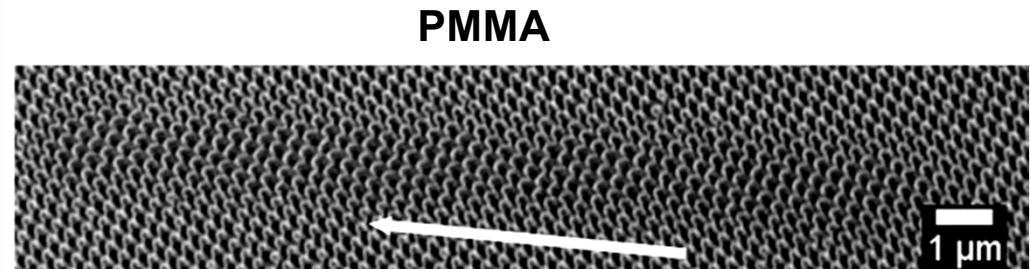
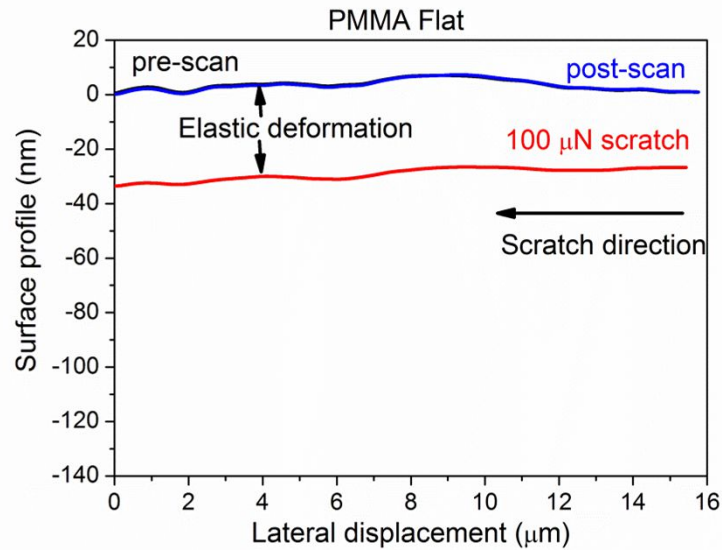
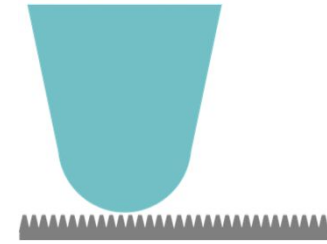
20 load/unload cycles until maximum load of 200 μN

Stiffness

Slope of the curves in the elastic region (maximum of 10 nm)

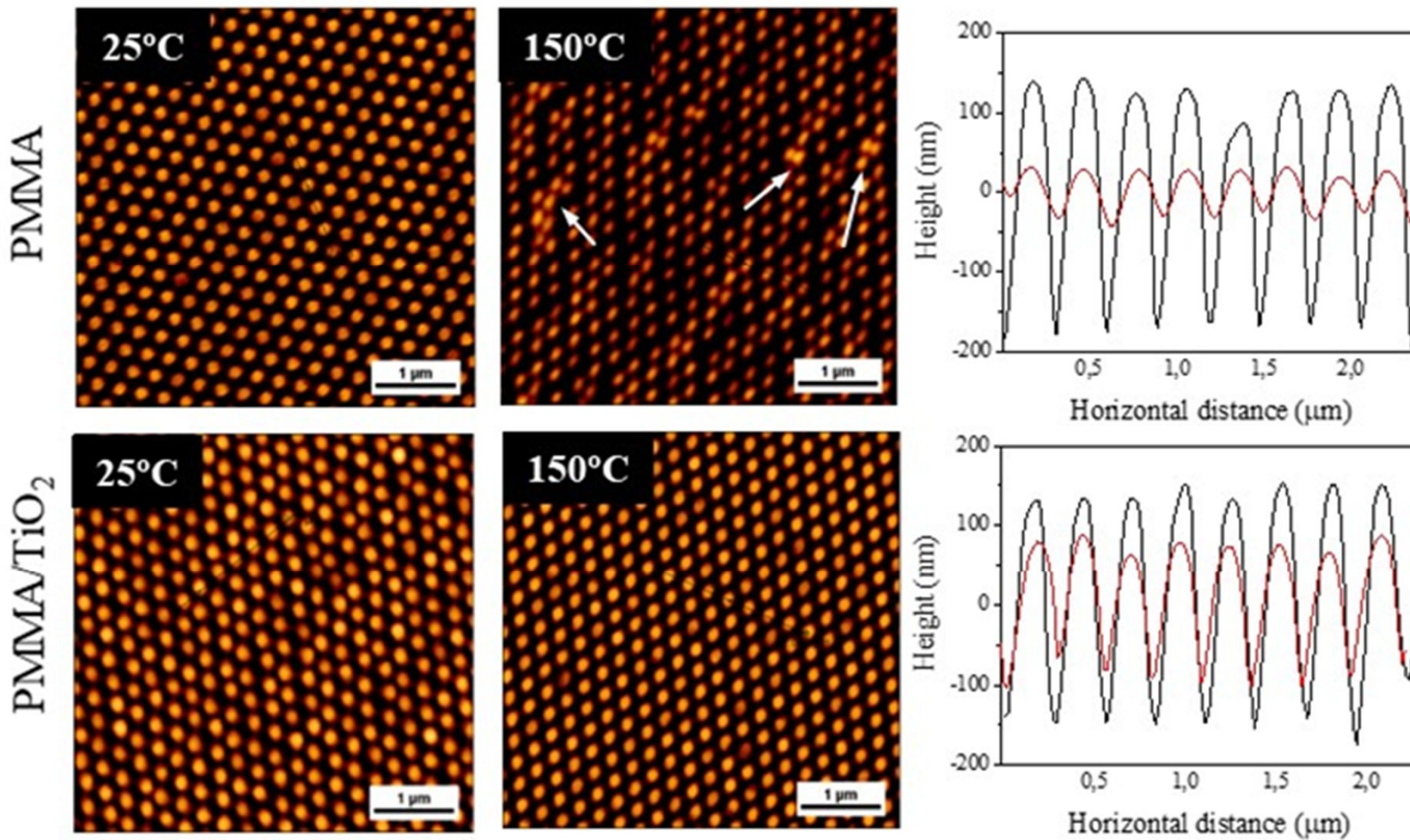


Mechanical behavior: Nanoscratch



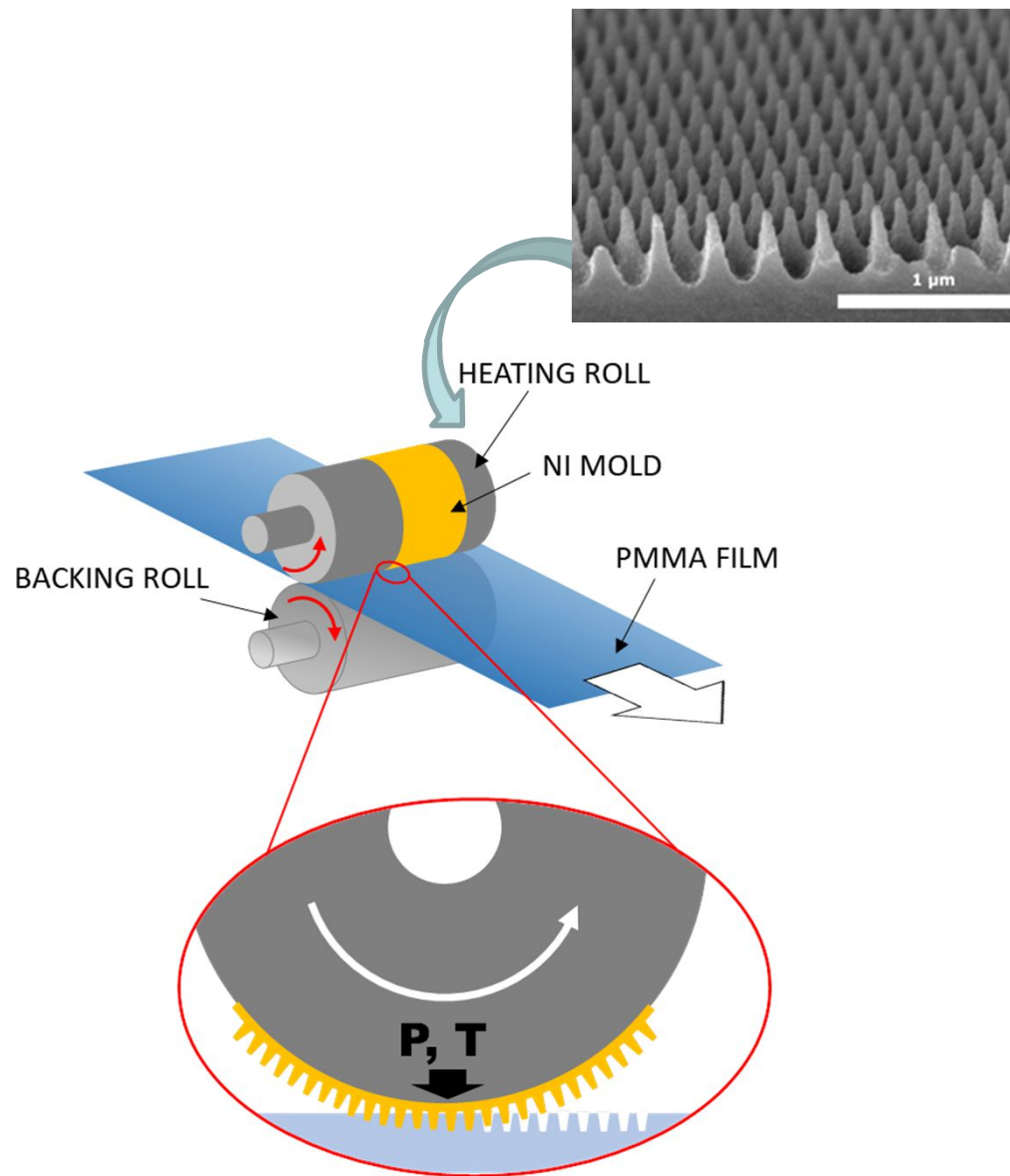
Improved thermal stability

Moth-eye PMMA/TiO₂ surface nanocomposites



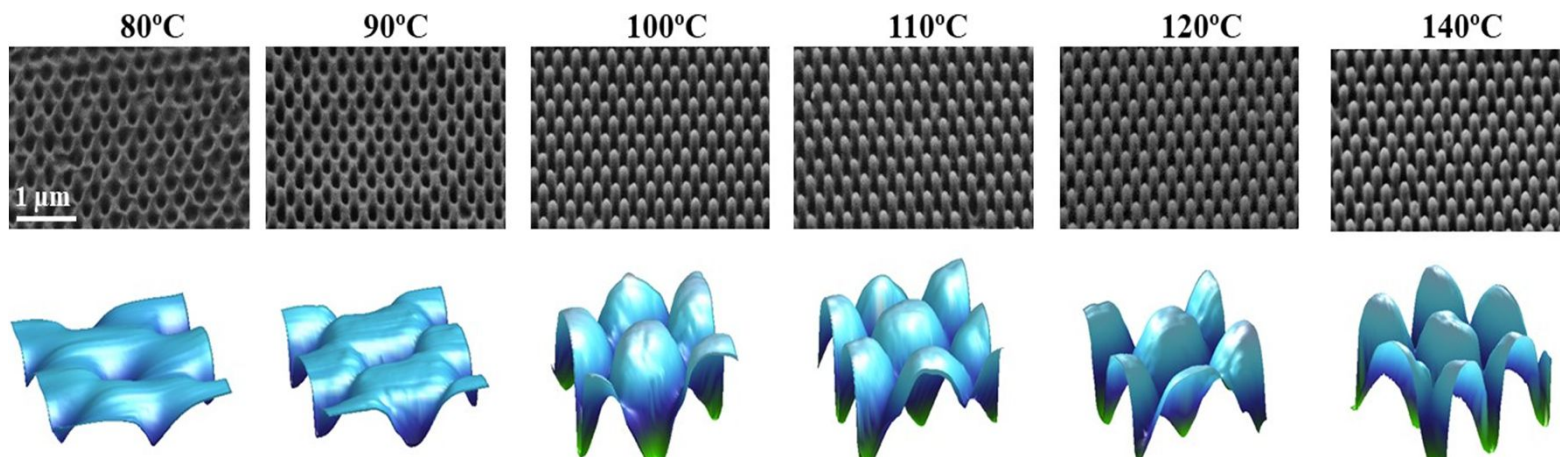
“anchoring effect of the TiO₂ NP to the polymer chain mobility” – pattern stability

Thermal R2R imprinting of moth-eye non-reflective films

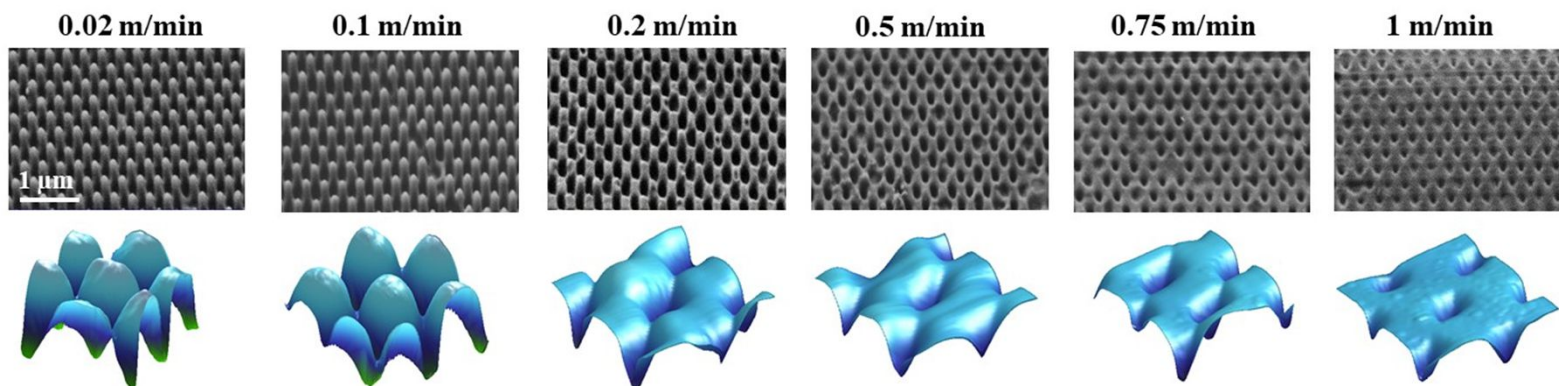


Thermal R2R imprinting of moth-eye non-reflective films

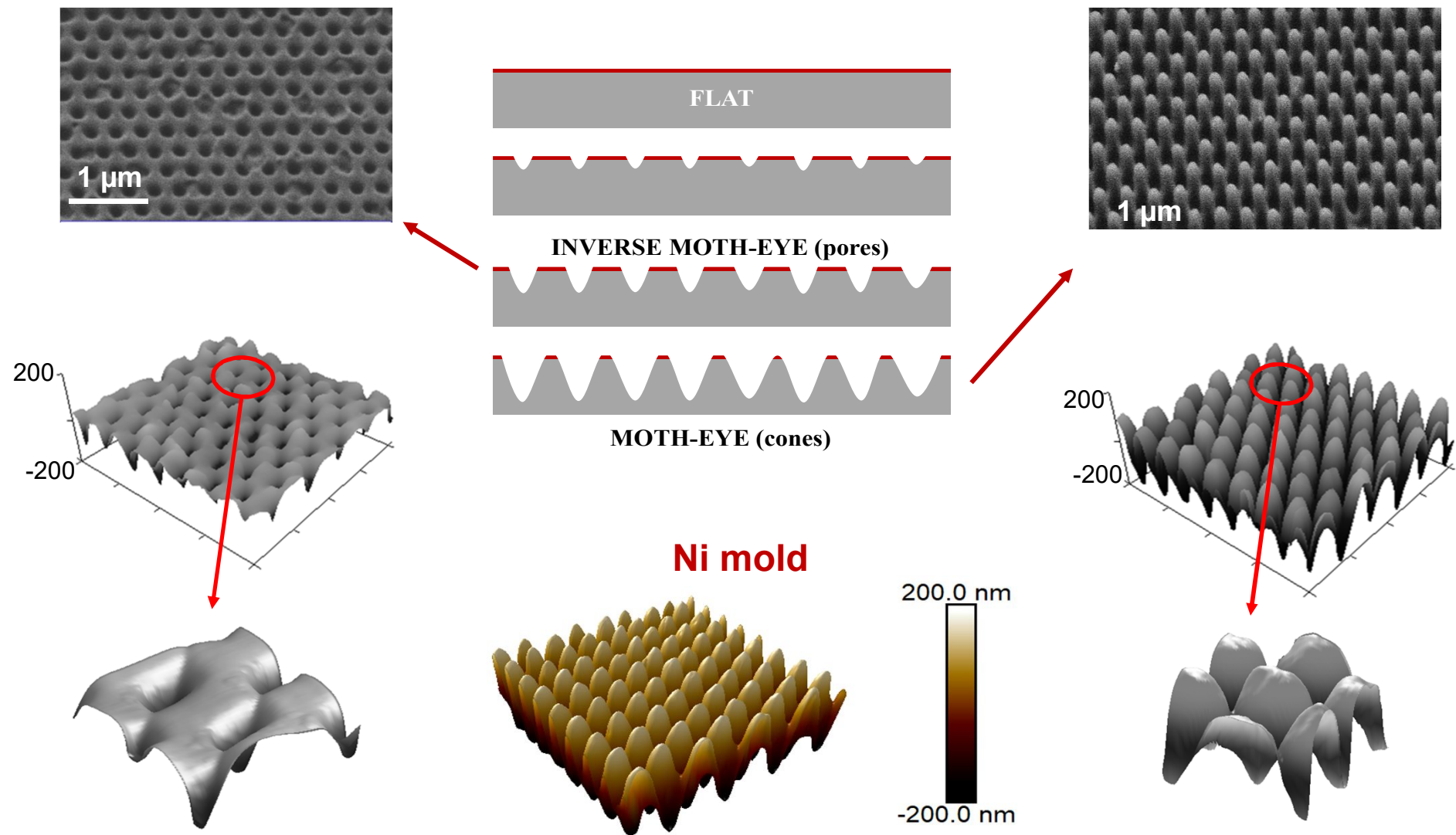
@ Variable temperature



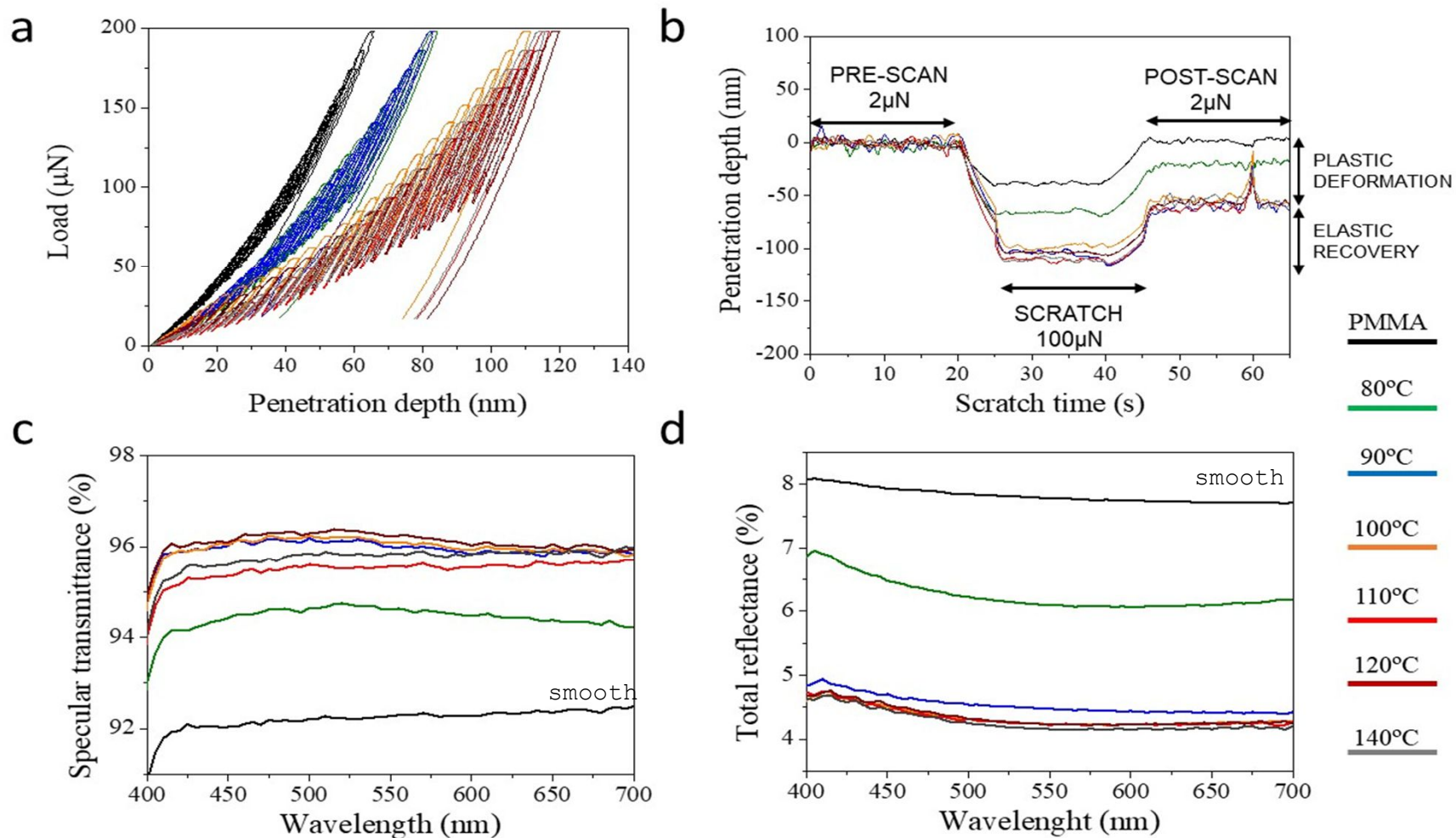
@ Variable speed



Thermal R2R imprinting of moth-eye non-reflective films



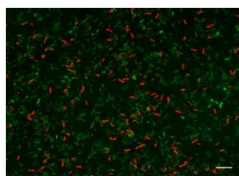
Thermal R2R imprinting of moth-eye non-reflective films



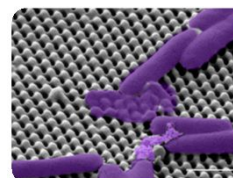
Bio-applications

1. Bactericidal Moth Eye Inspired Topography

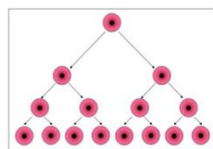
Fluorescence
Microscopy



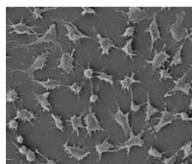
SEM



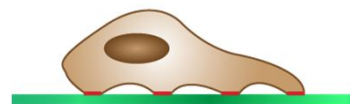
2. Cell Instructive Patterned Topographies



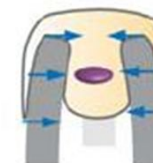
Proliferation



Morphology

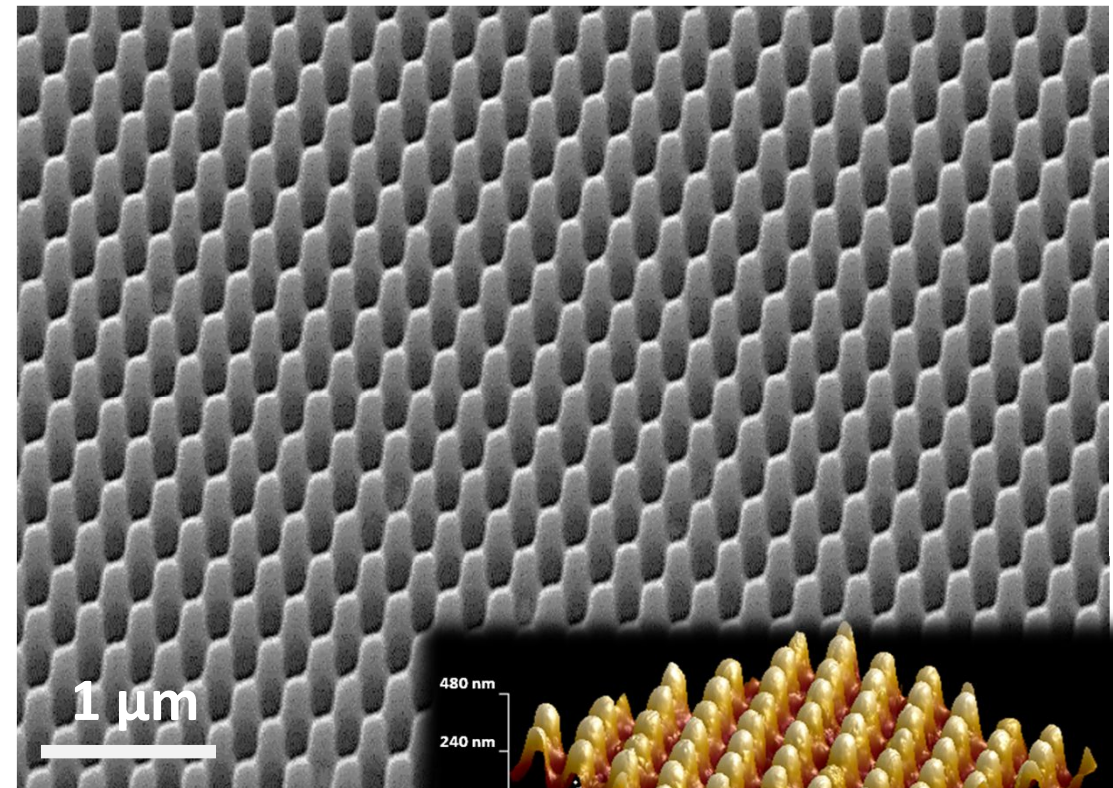
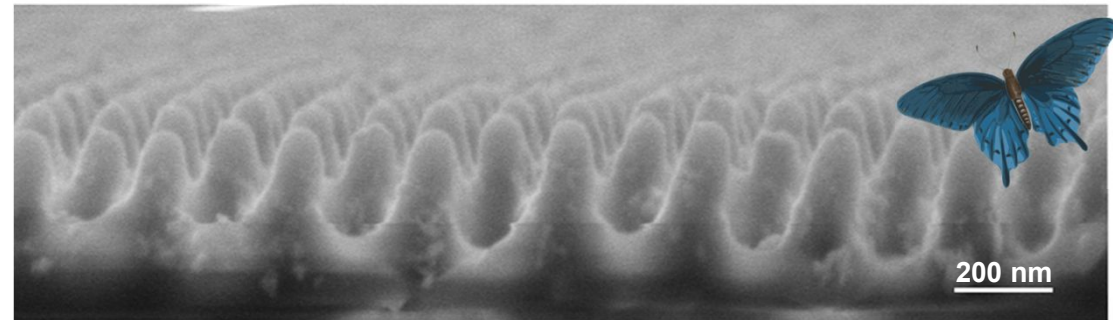
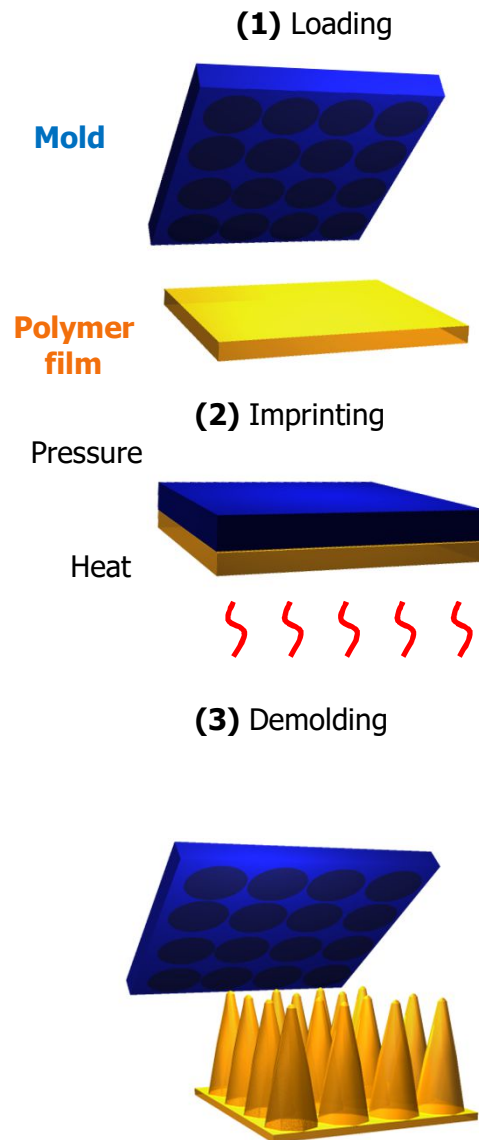


Migration

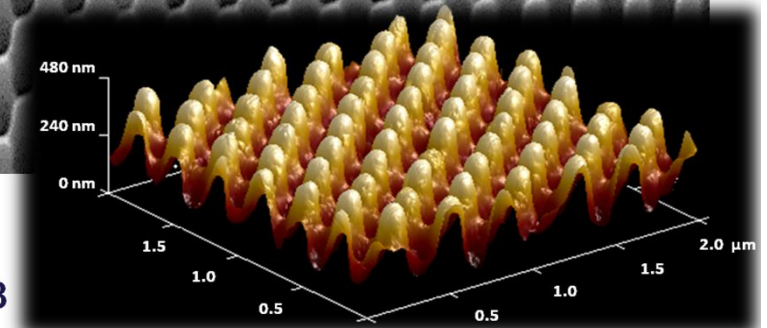


Cell Traction Force

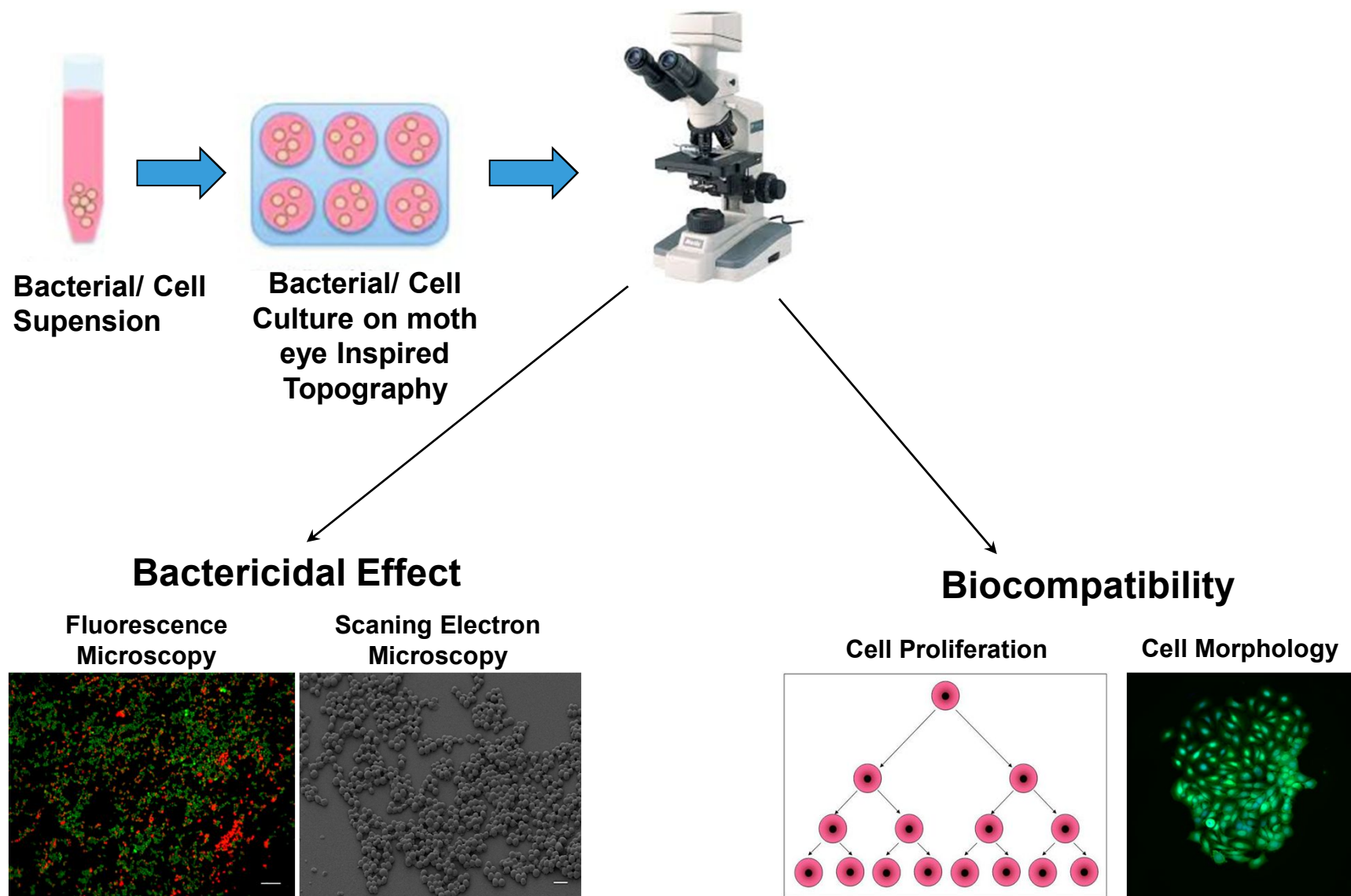
Moth-eye mimetic topography



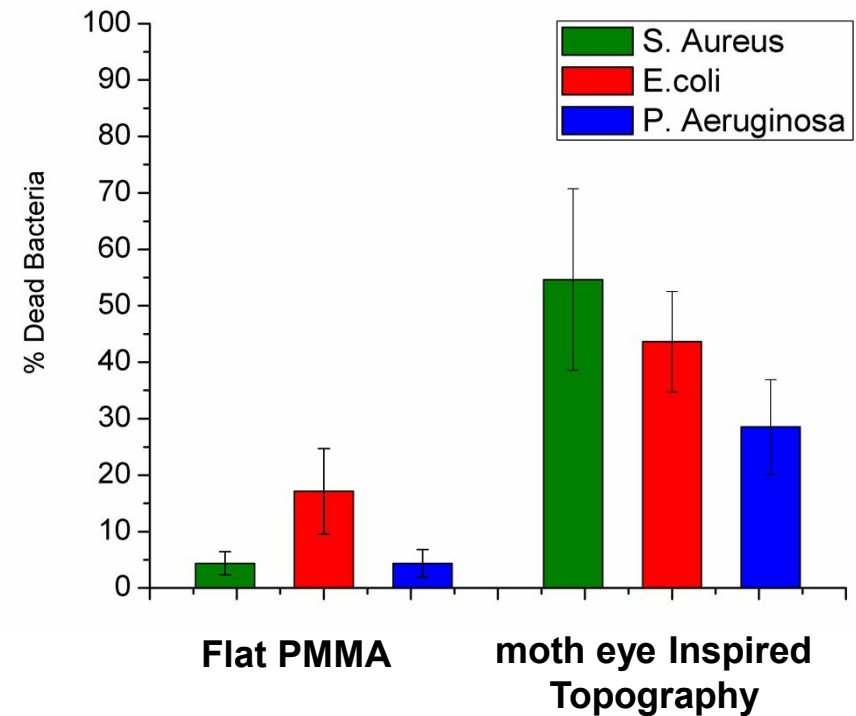
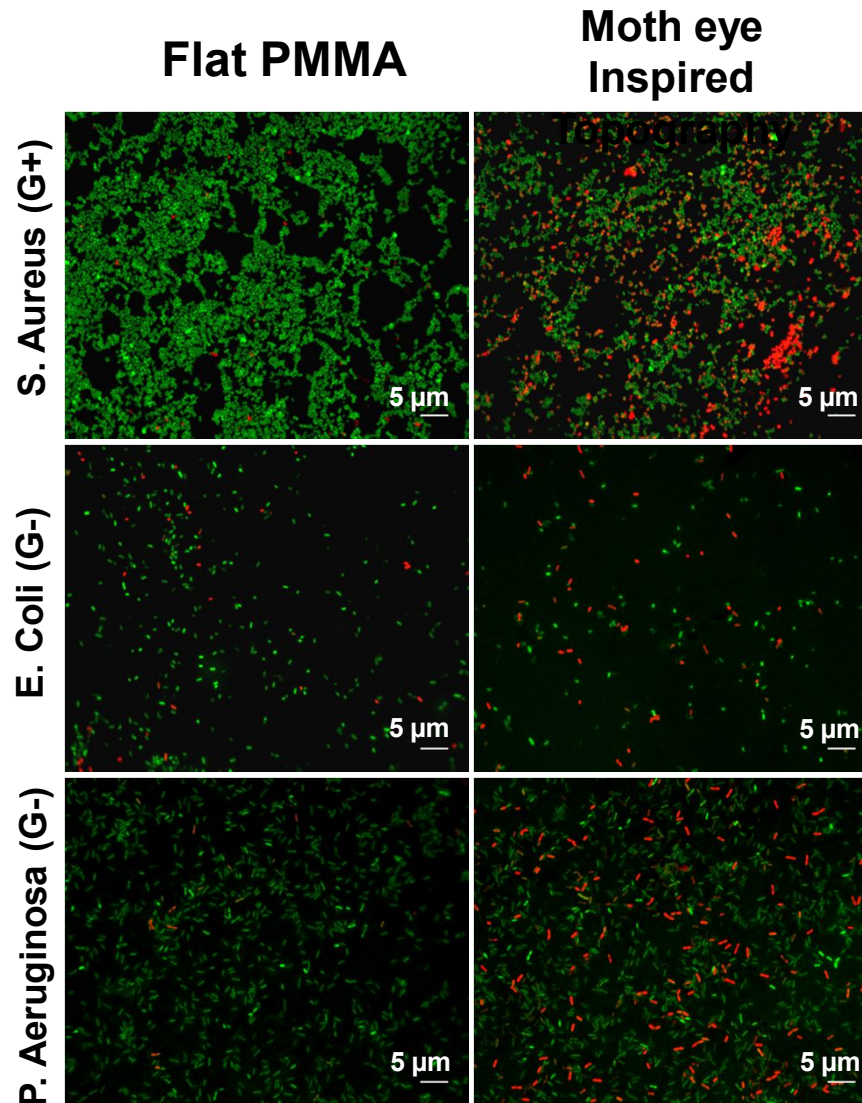
Height: 250 nm
Aspect Ratio: 2.8



EXPERIMENTAL SETUP

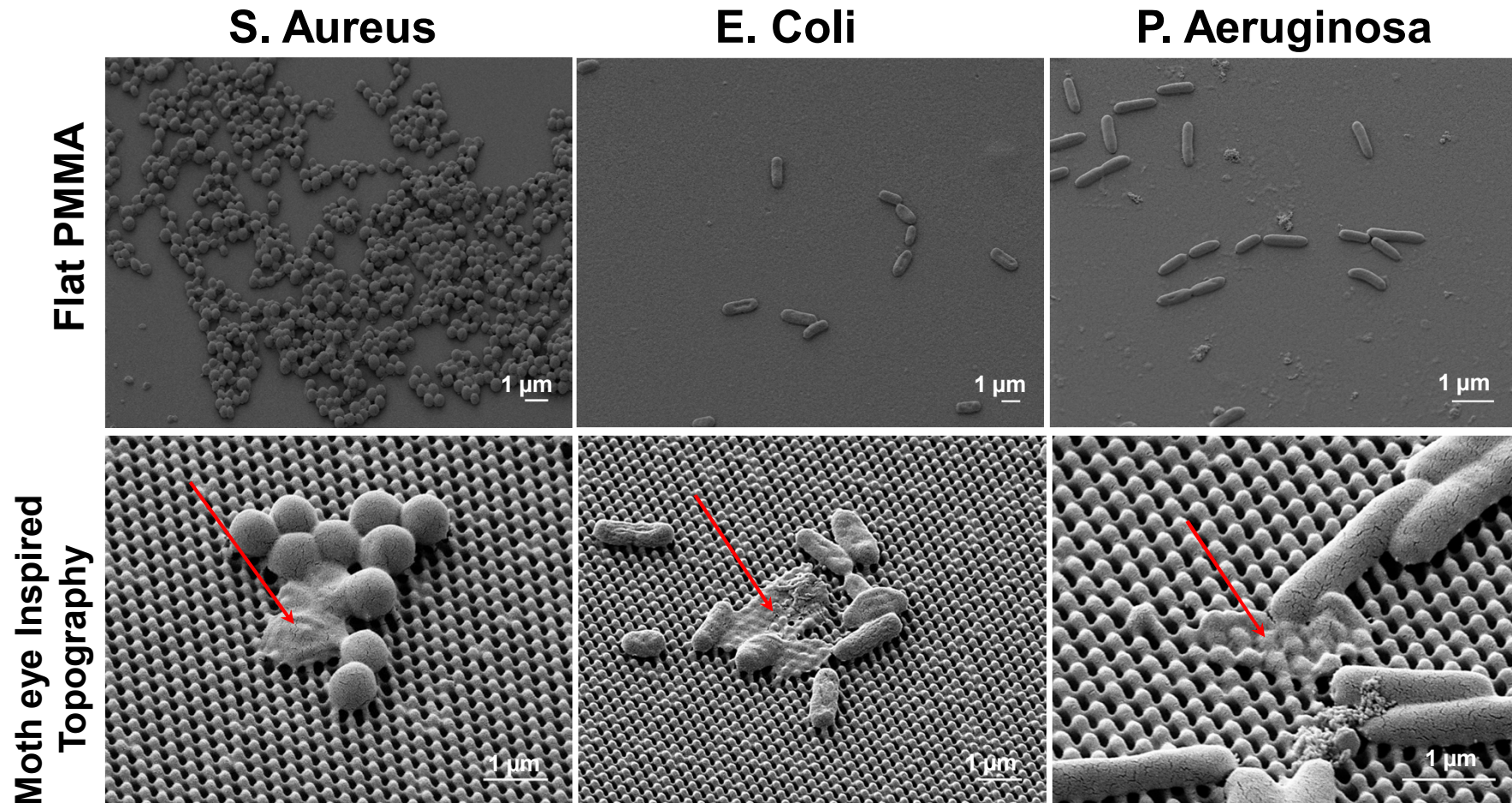


Bactericidal Efficacy of Moth Eye Topography



■ Live Bacteria
 ■ Dead Bacteria
 ■ Dead Bacteria

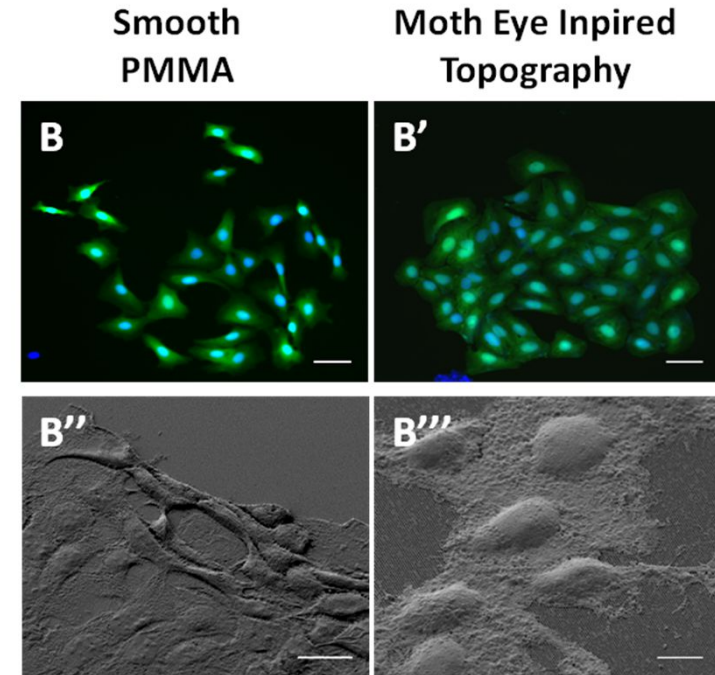
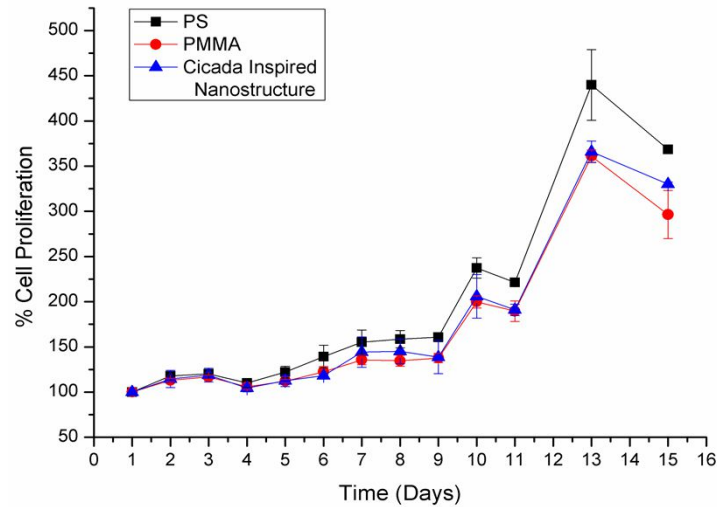
Moth Eye Bactericidal Effect



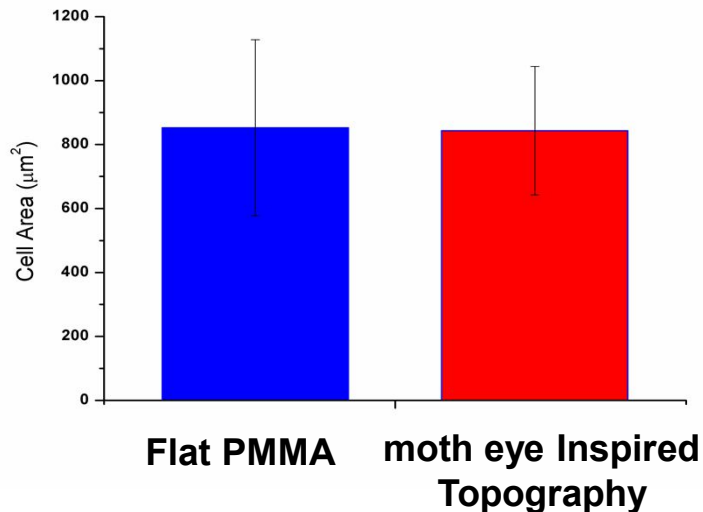
“Mechanical rupture – membrane stretching to optimize adhesion”

Biocompatibility of Moth Eye Topography

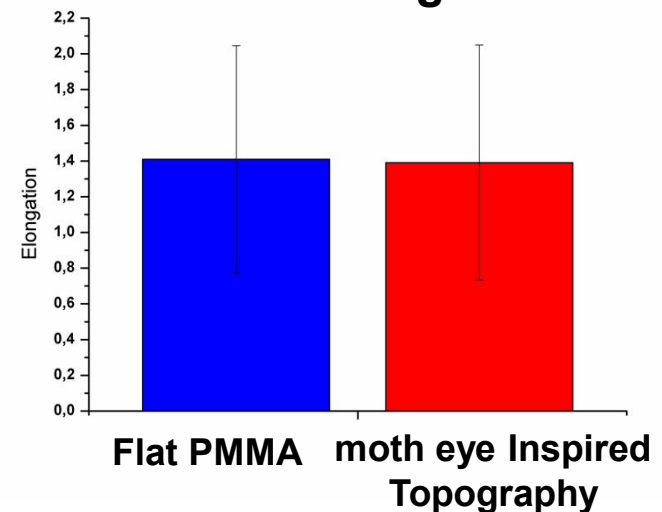
Cell Proliferation- HaCaT cells



Cell Spreading

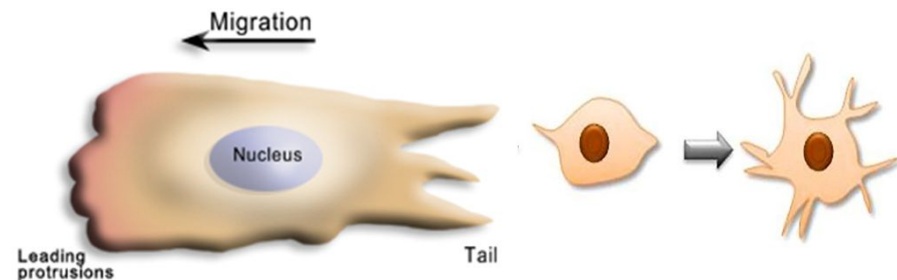
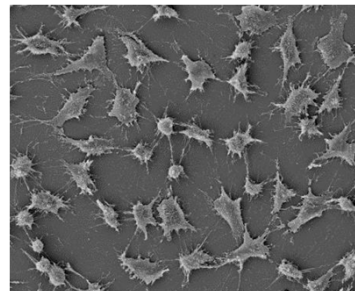
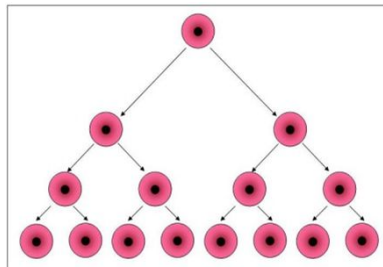
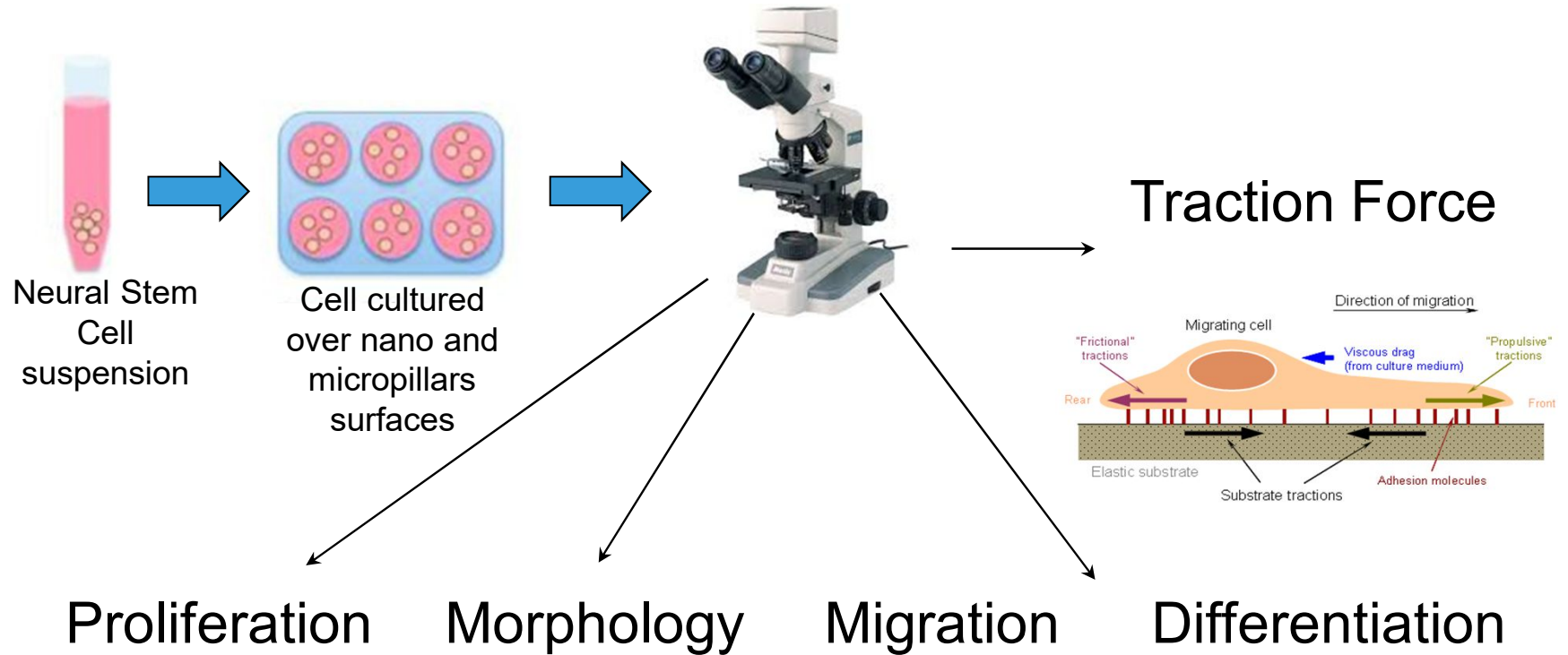


Cell Elongation



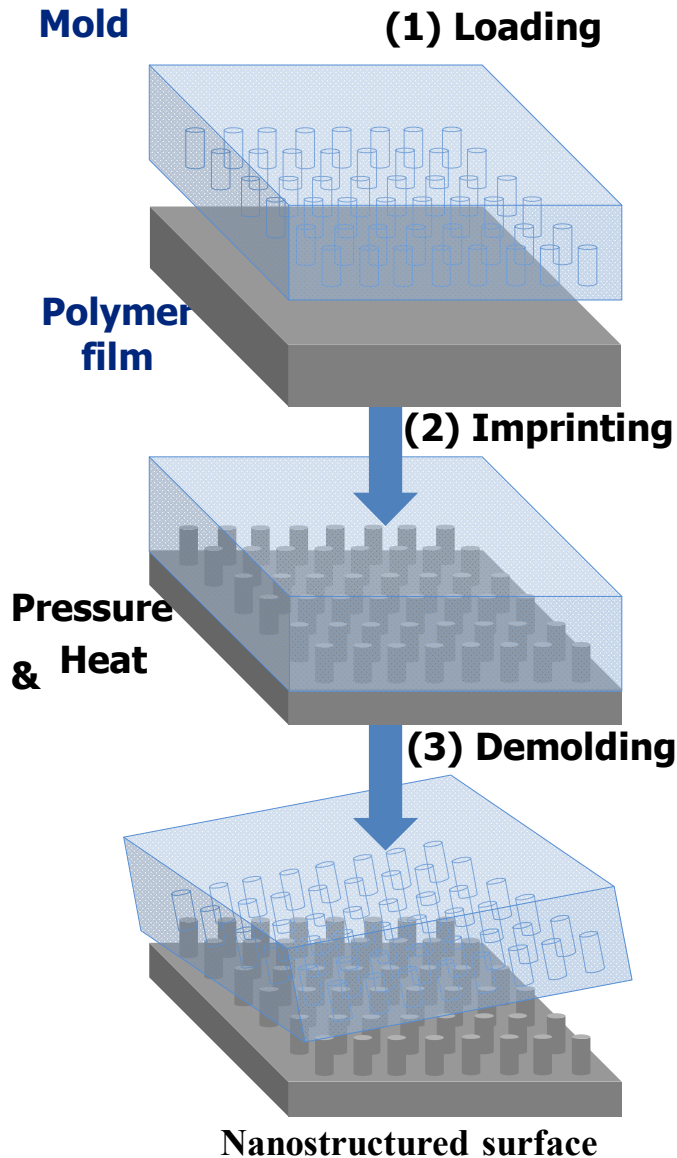
Cell Instructive Patterned Topographies

Experimental Setup



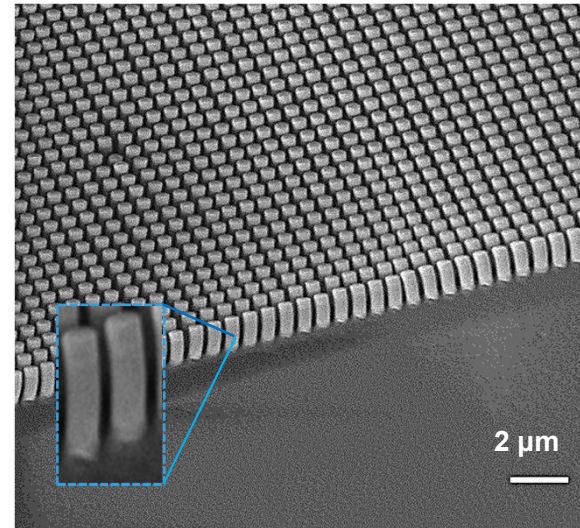
Polymer Nanoimprinting (NIL)

Replication technique: high fidelity, high resolution, low cost, scalable nanofabrication

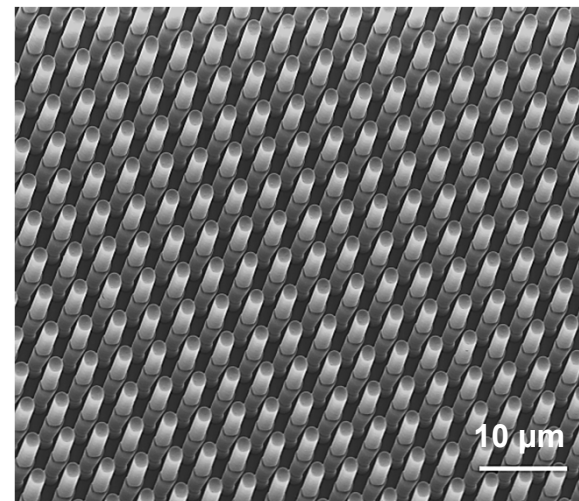


500 nm
pillars

2 μ m
pillars



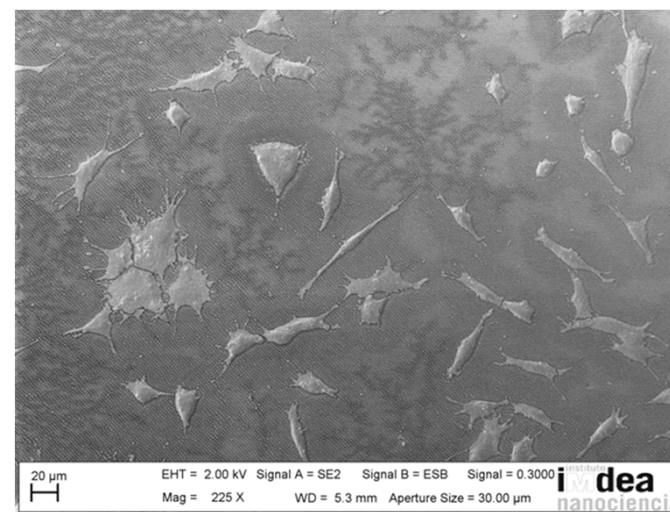
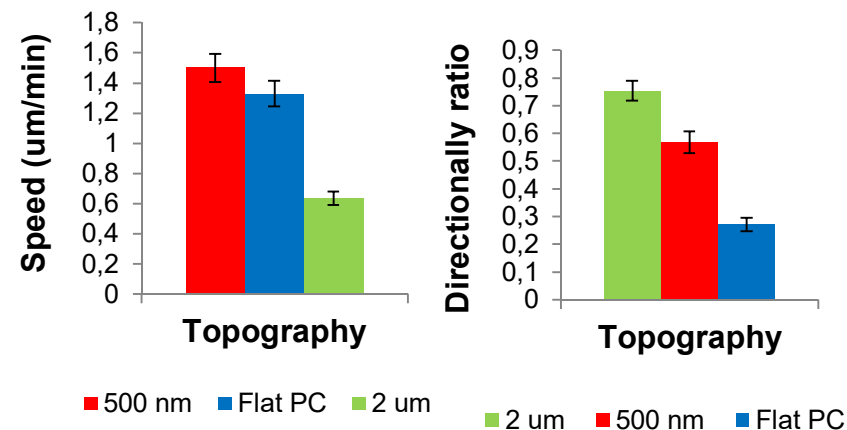
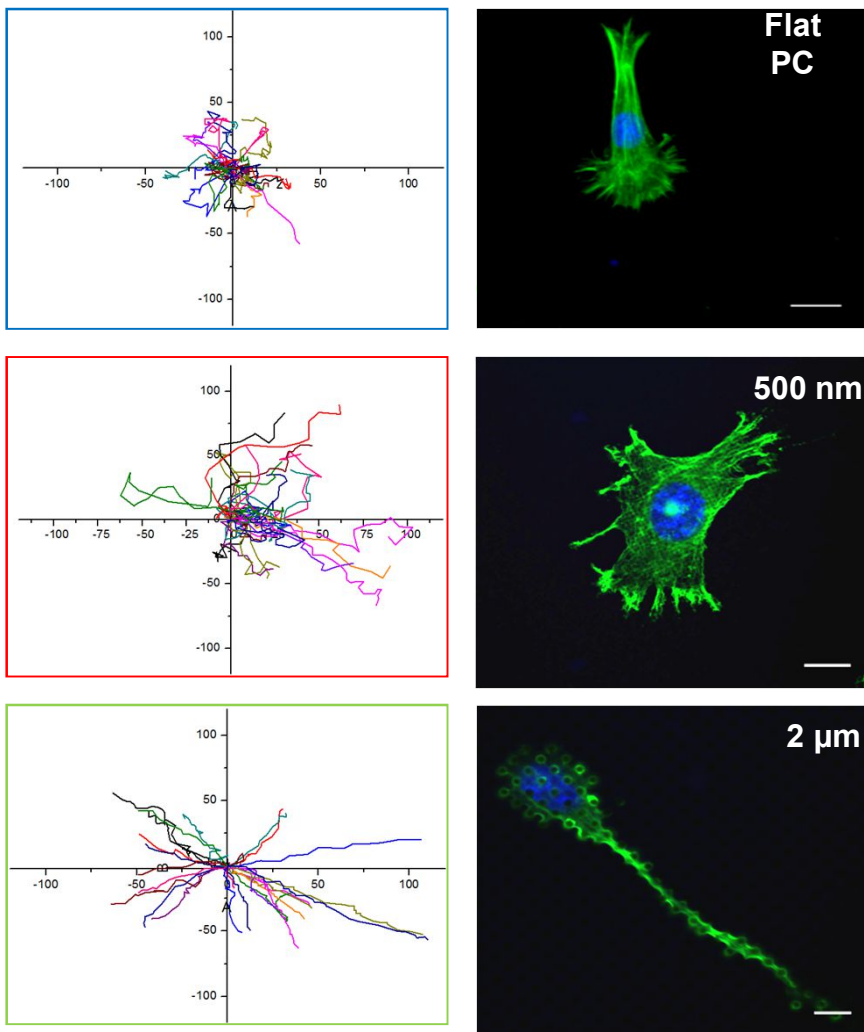
Diameter 500 nm
Height 2 μ m
Interpillar Gap
500 nm
Aspect Ratio 4



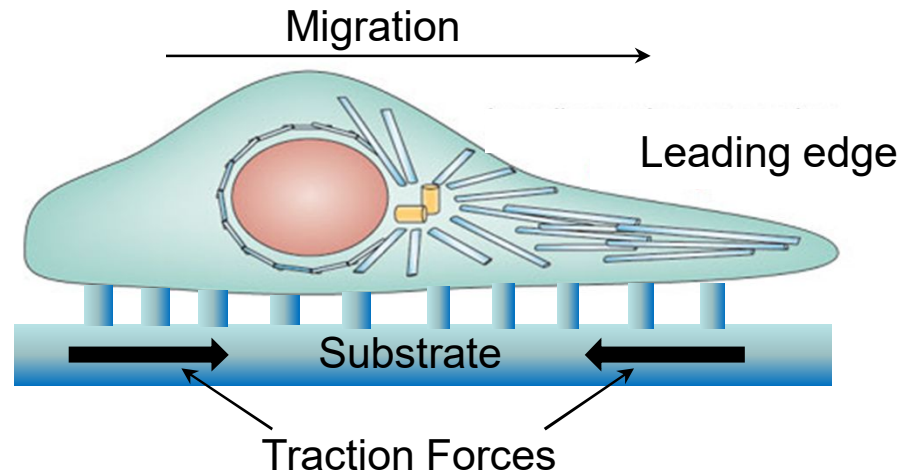
Diameter 2 μ m
Height 10 μ m
Interpillar Gap 2 μ m
Aspect Ratio 5

Cell Directional Migration

Windrose plots of cell trajectories

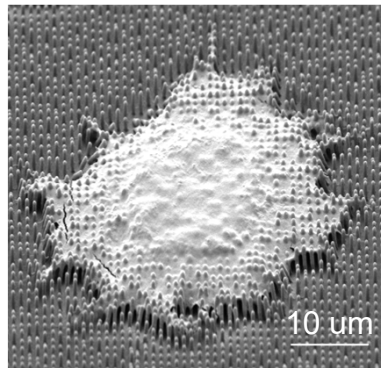


Cell Traction Force

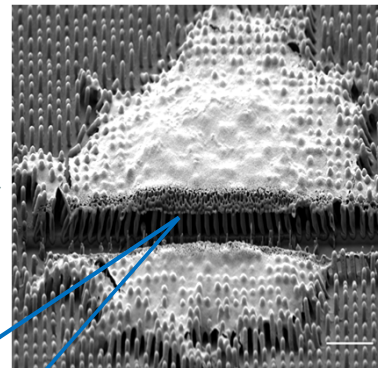


Hooke's Law
 $F = k\Delta x$

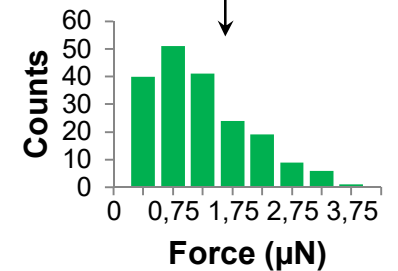
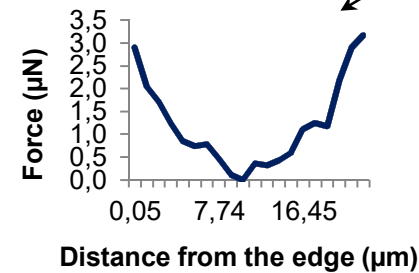
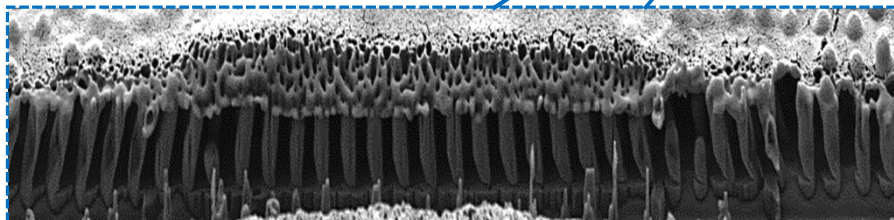
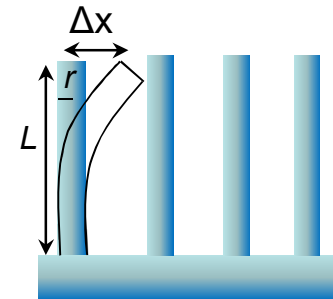
$$k = \frac{3}{4} \pi E \frac{r^4}{l^3}$$



FIB-SEM
Visualization

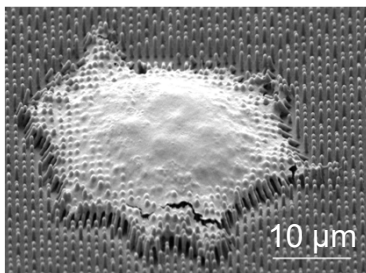


Bending angle
measurement

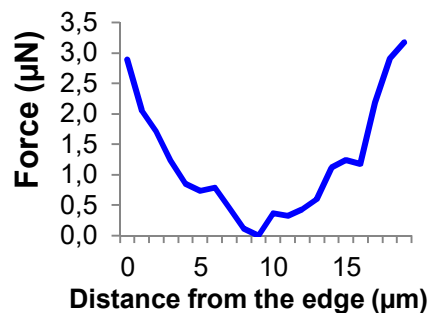


Cell Traction Force

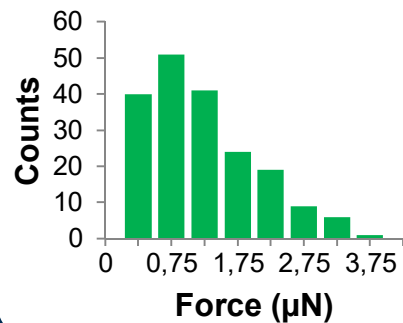
No Migration



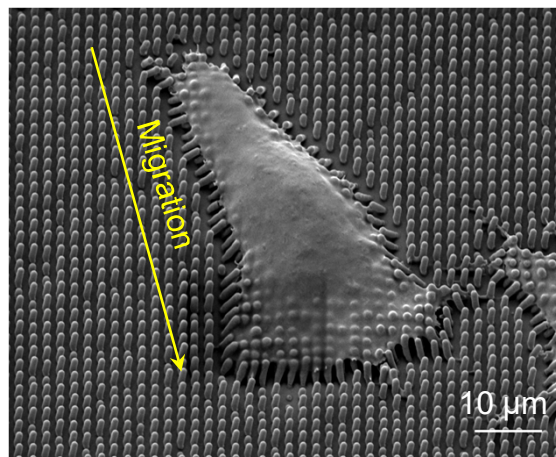
Single cell force profile



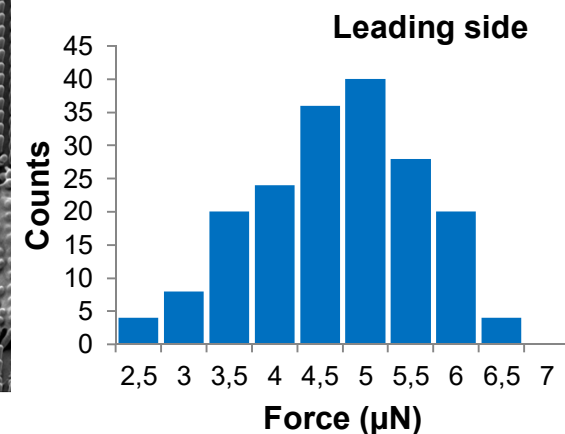
Mean force value



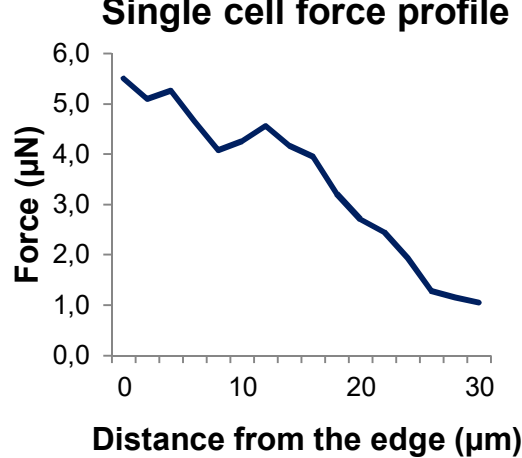
Migration



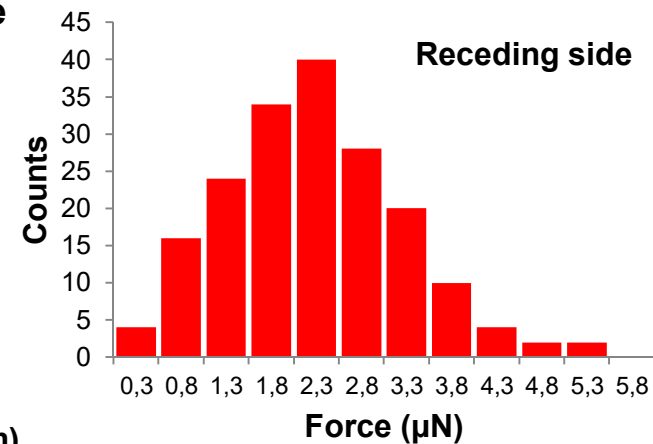
Mean force value



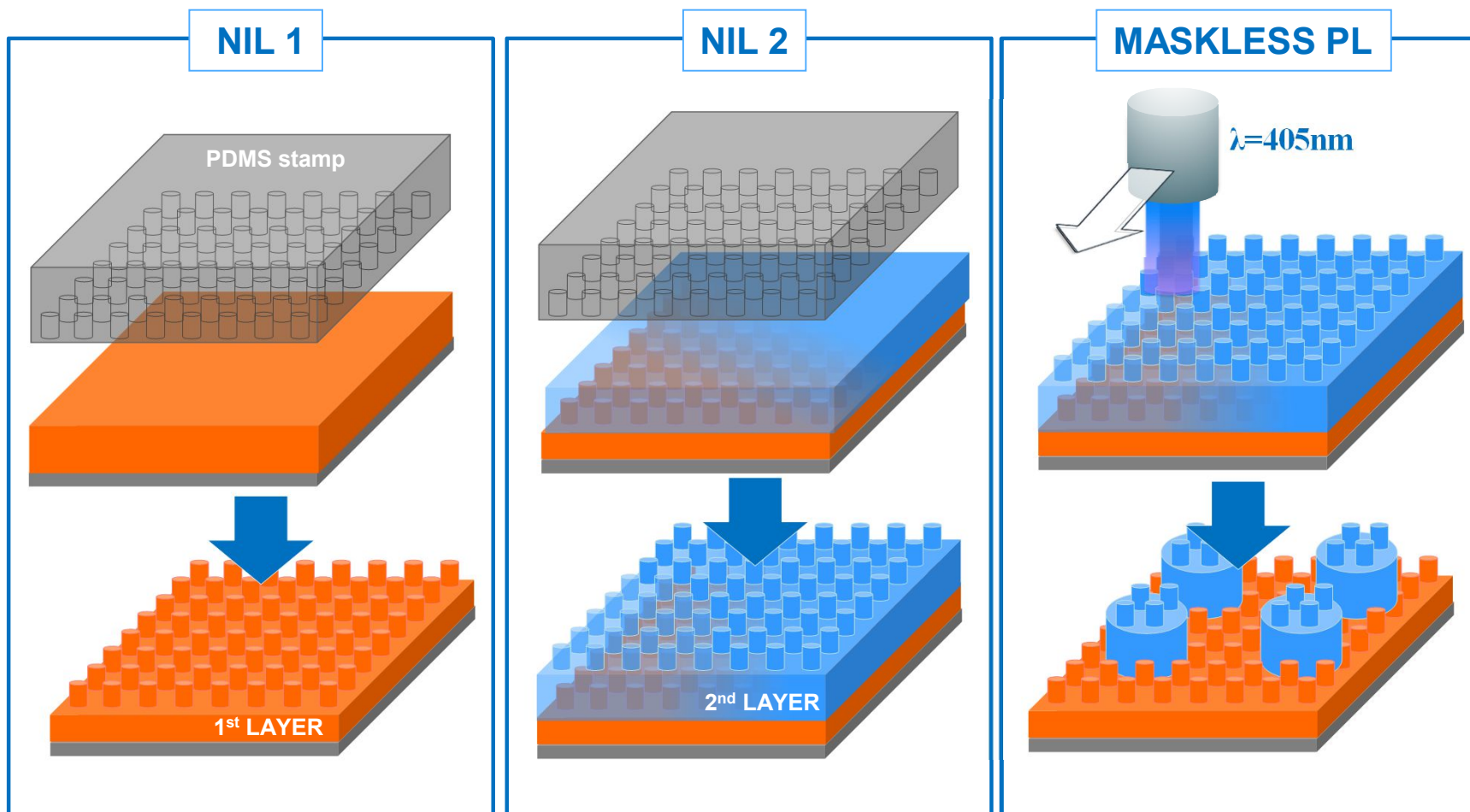
Single cell force profile



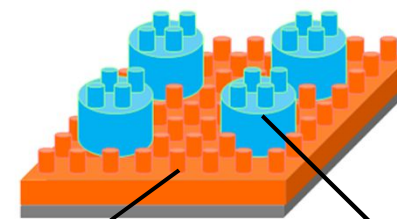
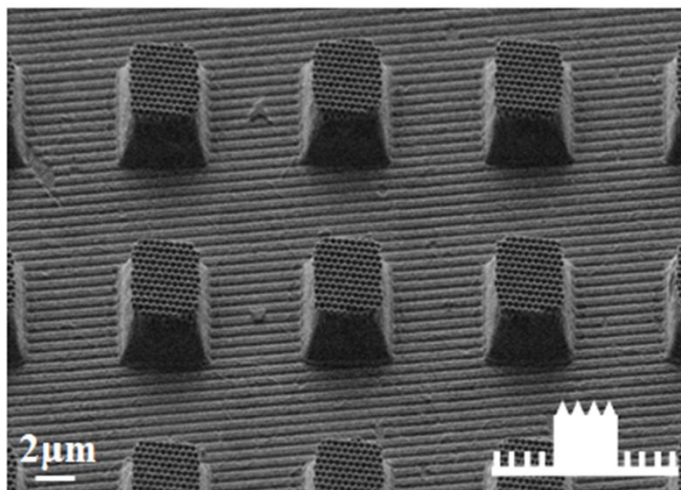
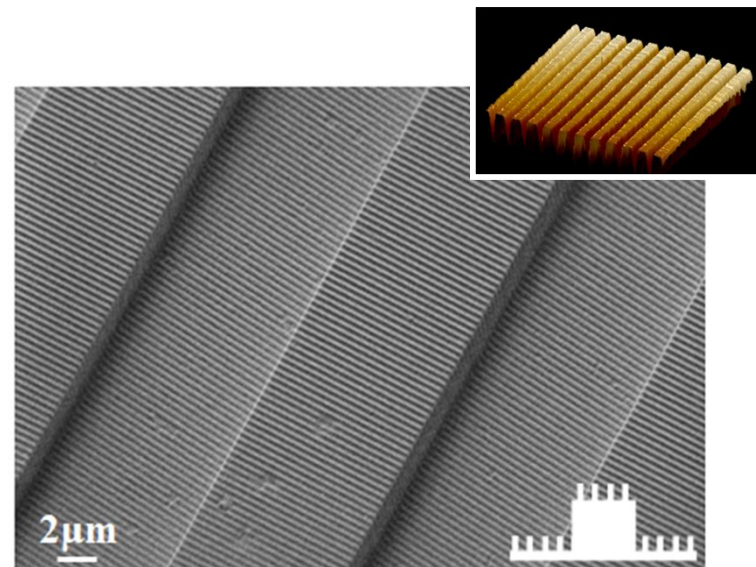
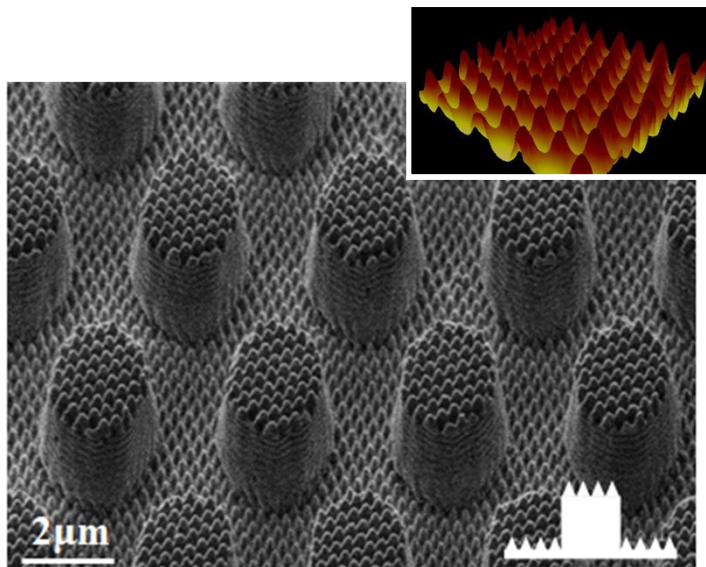
Mean force value



Novel fabrication procedure: NIL + PL



NIL: Nanoimprint Lithography ; PL: Photolithography



PMMA-A4
 $T_g = 98-106^\circ\text{C}$
 $T_{NIL} = 170^\circ\text{C}$
 $P_{NIL} = 30\text{bar}$
 $t = 5\text{min}$

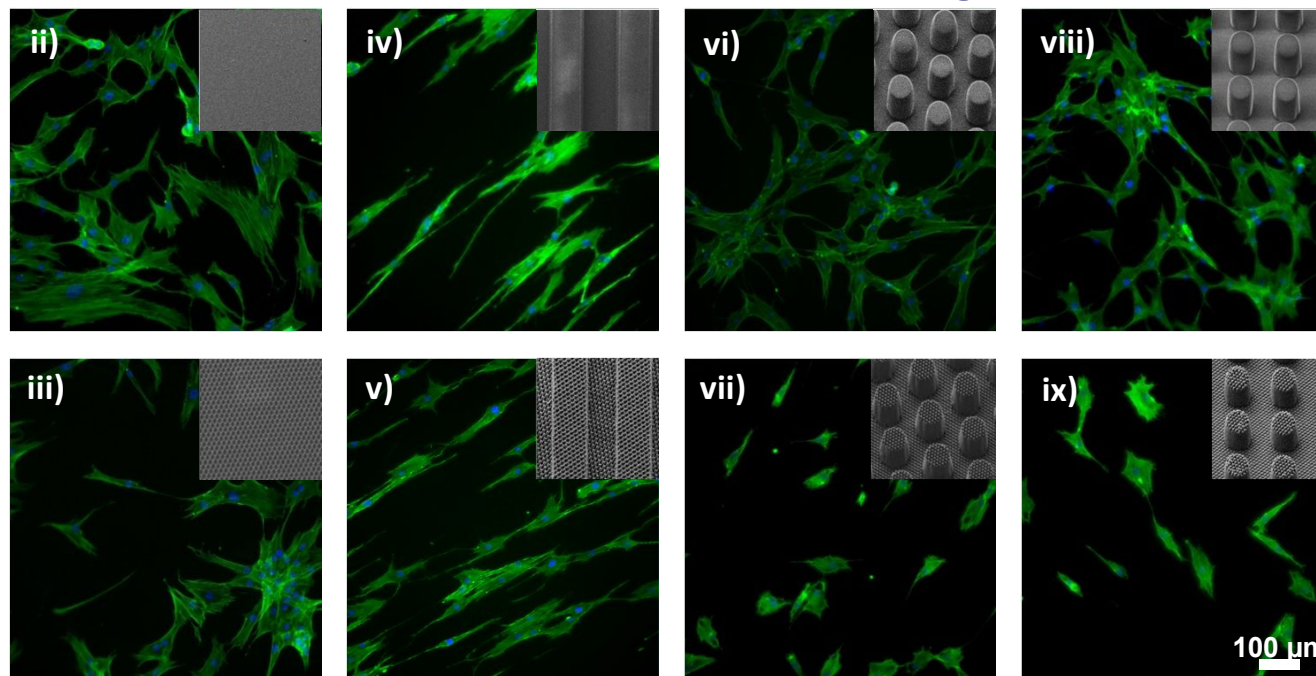
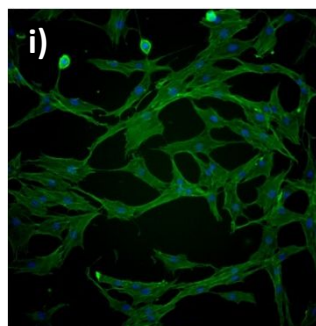
AZ1512
 S.C: 2000rpm, 1min
 $T_{NIL} = 100^\circ\text{C}$
 $P_{NIL} = 30\text{bar}$
 $t = 5\text{min}$

Mesenchymal stem cells (iAdMSC)

Attachment and cell morphology

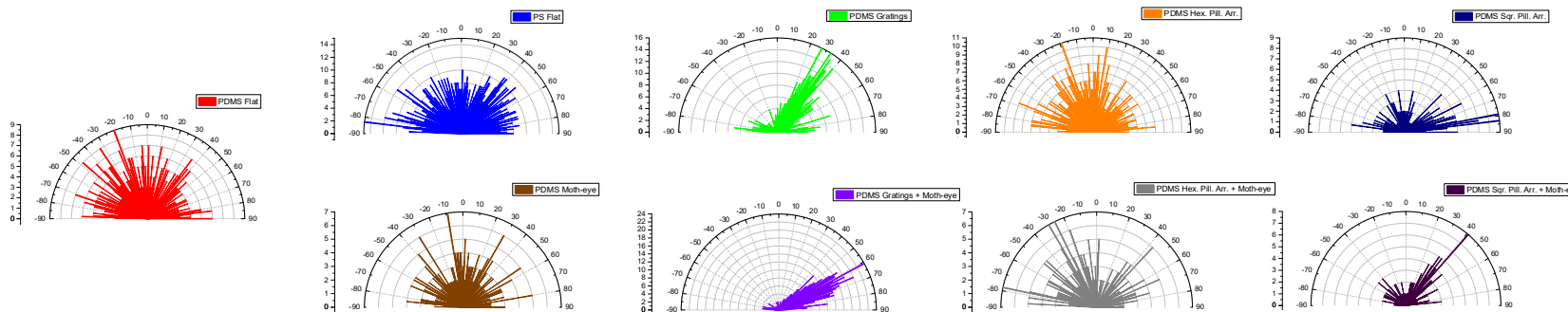
PDMS Micro-topographies

TCP -control

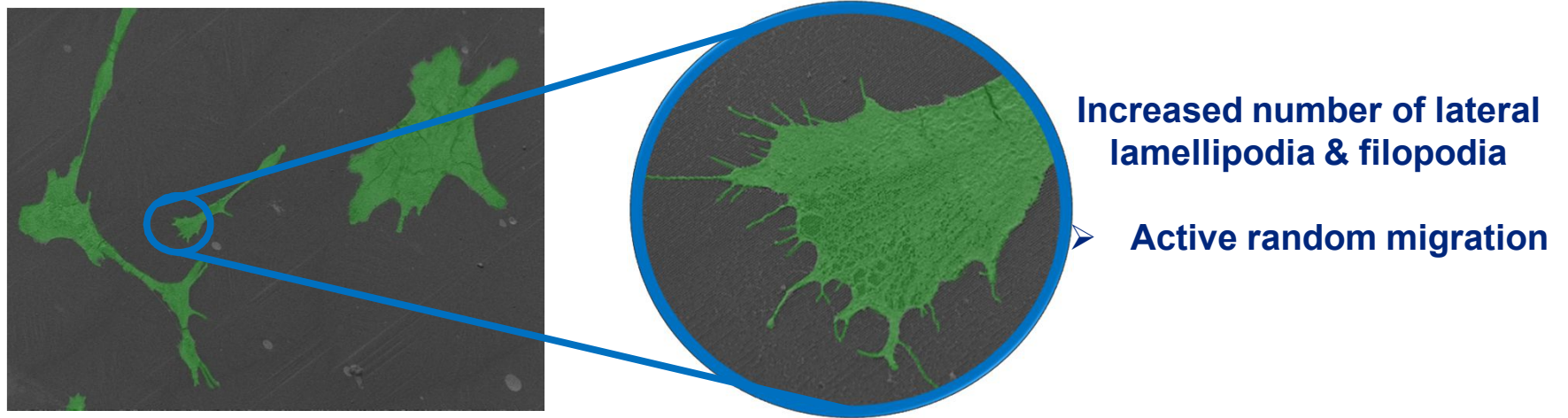


PDMS Hierarchical topographies

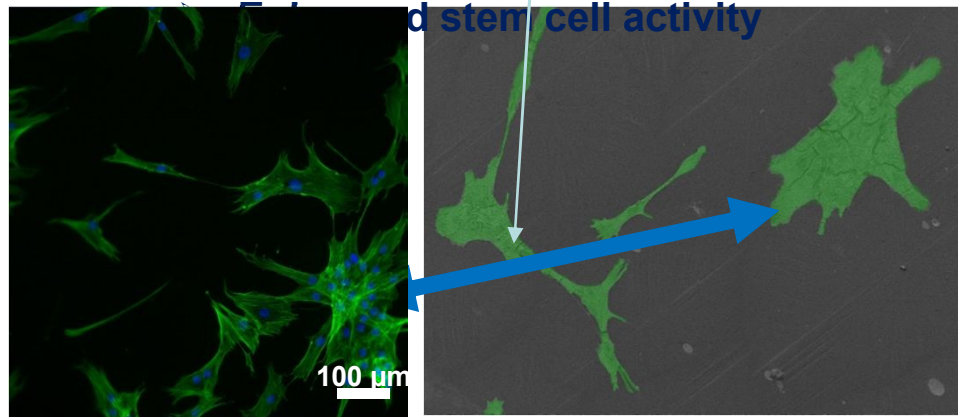
Orientation & spreading



MSC morphology on moth-eye & moth-eye hierarchies



Cell clusters' formation, increased cell-to-cell contact

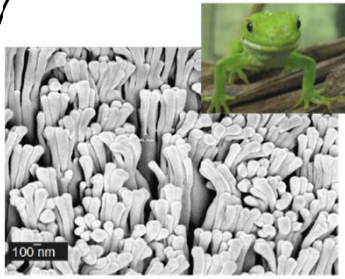


Osteogenic differentiation / Alizarin Red staining

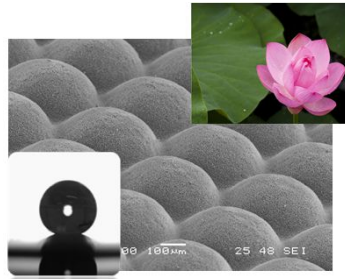


Summary

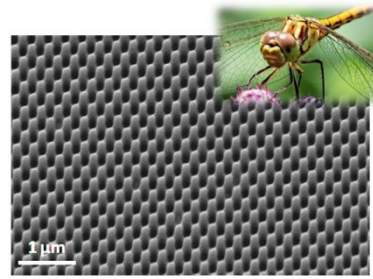
•Polymer micro/nano imprinting



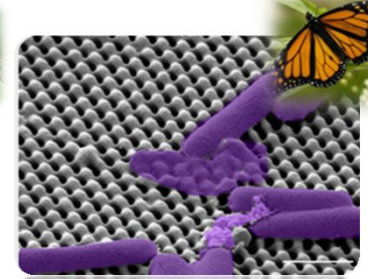
Gecko like dry adhesives



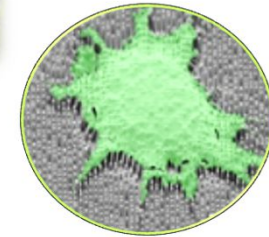
Superhydrophobic, self cleaning



Anti-reflective surfaces



Bactericidal surfaces



Cell substrates

- ❖ Patterning is a valuable tool to exploit the functionality of materials into new applications . Design is key to achieve specific functions.
- ❖ Structuring imparts function by physical means without the need for chemical modification. Lower developmental cost.
- ❖ Patterning -using replication (NIL) is a suitable methodology for **sustainable product development / nanomanufacturing**

References

- Book Nanofabrication: nanolithography techniques and their applications, J. M. De Teresa (editor), Chapter 7, Institute of Physics, UK (2020). Rodríguez, I., & Hernández, J. Soft thermal nanoimprint and hybrid processes to produce complex structures. Pages 7-1 to 7-33
- Schiff, H. and A. Kristensen, Nanoimprint lithography—patterning of resists using molding, in Springer Handbook of Nanotechnology. 2010, Springer. p. 271-312.
- Schiff, H. (2008). Nanoimprint lithography: An old story in modern times? A review. *Journal of Vacuum Science & Technology B: Microelectronics and Nanometer Structures Processing, Measurement, and Phenomena*, 26(2), 458-480.
- Ho, A. Y. Y., Yeo, L. P., Lam, Y. C., & Rodríguez, I. (2011). Fabrication and analysis of gecko-inspired hierarchical polymer nanosetae. *Acs Nano*, 5(3), 1897-1906.
- Ho, A. Y. Y., Luong Van, E., Lim, C. T., Natarajan, S., Elmouelhi, N., Low, H. Y., ... & Rodriguez, I. (2014). Lotus bioinspired superhydrophobic, self-cleaning surfaces from hierarchically assembled templates. *Journal of Polymer Science Part B: Polymer Physics*, 52(8), 603-609.
- Navarro-Baena, I., Jacobo-Martín, A., Hernández, J. J., Smirnov, J. R. C., Viela, F., Monclús, M. A., ... & Rodríguez, I. (2018). Single-imprint moth-eye anti-reflective and self-cleaning film with enhanced resistance. *Nanoscale*, 10(33), 15496-15504.
- Jacobo-Martín, A., Hernández, J. J., Pedraz, P., Solano, E., Navarro-Baena, I., & Rodríguez, I. (2021). Improved thermal stability of antireflective moth-eye topography imprinted on PMMA/TiO₂ surface nanocomposites. *Nanotechnology*, 32(33), 335302.
- Jacobo-Martín, A., Rueda, M., Hernández, J. J., Navarro-Baena, I., Monclús, M. A., Molina-Aldareguia, J. M., & Rodríguez, I. (2021). Bioinspired antireflective flexible films with optimized mechanical resistance fabricated by roll to roll thermal nanoimprint. *Scientific reports*, 11(1), 1-15.
- Viela, F., Navarro-Baena, I., Hernández, J. J., Osorio, M. R., & Rodríguez, I. (2018). Moth-eye mimetic cytocompatible bactericidal nanotopography: a convergent design. *Bioinspiration & biomimetics*, 13(2), 026011.
- Viela, F., Granados, D., Ayuso-Sacido, A., & Rodríguez, I. (2016). Biomechanical cell regulation by high aspect ratio nanoimprinted pillars. *Advanced Functional Materials*, 26(31), 5599-5609.
- Alameda, M. T., Osorio, M. R., Hernández, J. J., & Rodríguez, I. (2019). Multilevel Hierarchical Topographies by Combined Photolithography and Nanoimprinting Processes To Create Surfaces with Controlled Wetting. *ACS Applied Nano Materials*, 2(8), 4727-4733.

Acknowledgements



Alejandra Jacobo
Jaime Hernandez
Maria Teresa Alameda
Felipe Viela
Ivan Navarro
Alberto Martín Asensio
Sergio Dávila
Miguel Esteban Lucía
Manuel R Osorio
Daniel Granados

Jon Molina
Miguel Monclus

Audrey Ho
Emma van Luong
Low Hong Yee



IMRE